

Chemical Science

Accepted Manuscript

This article can be cited before page numbers have been issued, to do this please use: P. Innocenzi and L. Stagi, *Chem. Sci.*, 2020, DOI: 10.1039/D0SC02658A.



This is an Accepted Manuscript, which has been through the Royal Society of Chemistry peer review process and has been accepted for publication.

Accepted Manuscripts are published online shortly after acceptance, before technical editing, formatting and proof reading. Using this free service, authors can make their results available to the community, in citable form, before we publish the edited article. We will replace this Accepted Manuscript with the edited and formatted Advance Article as soon as it is available.

You can find more information about Accepted Manuscripts in the [Information for Authors](#).

Please note that technical editing may introduce minor changes to the text and/or graphics, which may alter content. The journal's standard [Terms & Conditions](#) and the [Ethical guidelines](#) still apply. In no event shall the Royal Society of Chemistry be held responsible for any errors or omissions in this Accepted Manuscript or any consequences arising from the use of any information it contains.

Carbon-based Antiviral Nanomaterials, Graphene, C-dots, Fullerenes. A perspective

View Article Online
DOI: 10.1039/D0SC02658A

Plinio Innocenzi, Luigi Stagi

Department of Chemistry and Pharmacy, Laboratory of Materials Science and Nanotechnology,
CR-INSTM, University of Sassari, via Vienna 2, 07100, Sassari, Italy

Abstract

The appearance of new and lethal viruses and their potential threat urgently requires innovative antiviral systems. In addition to the most common and proven pharmacological methods, nanomaterials can represent alternative resources to fight viruses at different stages of infection, by a selective action or in a broad spectrum. A fundamental requirement is non-toxicity. However, biocompatible nanomaterials have very often little or no antiviral activity, preventing their practical use. Carbon-based nanomaterials have displayed encouraging results and can represent the required mix of biocompatible and antiviral properties. In the present review, the main candidates for future carbon nanometric antiviral systems, namely graphene, carbon dots and fullerenes, have been critically analysed. In general, different carbon nanostructures allow several strategies to be applied. Some of the materials have peculiar antiviral properties, such as the singlet oxygen emission, or the capacity to interfere with the virus enzymes. In other cases, the nanomaterials have used as a platform for functional molecules able to capture and inhibit the viral activity. The use of carbon-based biocompatible nanomaterial as antivirals is still an almost unexplored field while the published results show promising perspectives.

1. Introduction

The Covid-19 viral infection, which has become one of the major threats to human health from 1918 flu pandemic, has urgently risen the need of antiviral drugs and vaccines. The time to develop them are, however, quite long and requires several phases before being approved to use in humans. In perspective, would be important developing innovative and long-term strategies to complement the existing pharmacological approaches to fight infections and specific viruses. Despite the great advances in technology, human beings often find themselves helpless in the face of new dangers arising from the emergence of new viruses. Viruses are the cause of about one third of deaths from infectious diseases¹. The lack of tools to fight virulent infections or the slow response to the outbreak of a pandemic can have catastrophic economic and social implications. Unfortunately, the only resource to counteract the development of viral infections is the use of vaccines, often employed when the infection is already widespread. Besides that, the few strategies we possess are antiviral drugs, symptom treatment, and isolation. Beyond the urgency to reduce and stop the pandemic it is also necessary to develop a new generation of antiviral tools which are as much possible flexible and show a broad range antiviral activity. Viruses are characterized by well-defined shapes and dimensions, which are in the nanoscale, and as such they could be also considered a kind of nanomaterial itself. Highly symmetric nanostructures, such as the fullerenes, have, for instance extraordinary geometric affinity with icosahedral viruses². The possibility of creating nanomaterials on the same scale and with similar geometry is a fascinating possibility. The similarities can



be used to foster the interactions and building smart nanostructures that can inhibit or inactivate virus replication. View Article Online
DOI: 10.1039/D0SC02658A

Antiviral substances can generally be divided into virostatic and virucidal, depending on the counteracting action against a particular virus¹. The former are substances that act in the early stages of infection by inhibiting viral replication and the proliferation of the virus. They are based on a binding mechanism and can, therefore, often be ineffective if they detach and leave the viral particles untouched¹. Virucidal medicines, on the other hand, can permanently deactivate the virus, with effects that remain even after dilution. However, many of the molecules that have such an effective antiviral action are toxic¹. Research on the antiviral properties of carbon-based nanomaterials is still in its embryonic state. The main interest in these systems lies precisely in their potential low toxicity³ and innovative virus inhibition mechanisms. The ambition of using nanoscale systems is to combine virostatic properties with virucidal inactivation processes.

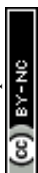
Among the nanomaterials that have been tested in nanomedicine and biotechnology, nanoparticles are certainly the most important to date⁴⁻⁶. The antiviral activity is exerted through multiple mechanisms. The small size and tailored functionalization of the surface allow favouring drug delivery and entry through the cell membrane (negatively charged). They can also have biomimetic properties as in the case of dendrimers¹. The possibilities of using nanomaterials for nanomedical purposes are potentially vast and take advantage of the flexible synthesis, biocompatibility, surface tunability, and design of the chemical and structural composition⁴.

In this perspective review, we have considered the most significant results in the field of carbon-based nanomaterials for antiviral applications. In general, carbon nanomaterials show low cytotoxicity and present specific antiviral activities. Although relatively new in the nanomedical field, they have boosted an intense research activity aimed at controlling synthesis and functionalization of the surfaces. The related surface engineering has allowed an effective tuning of the surface properties for specific applications. Graphene-based systems have proven to work well both via direct interaction with the virus (also through photo-induced mechanisms) and as platforms for other particles or molecules with antiviral properties. In addition to graphene also carbon dots, systems smaller than 10 nm, have been shown specific antiviral properties and broad-spectrum responses. The other class of carbon nanomaterials that we have considered is fullerene and its derivatives. They have been the first one to be tested as antiviral carbon materials and have shown remarkable antiviral properties as an inhibitor of the viral activity or as a photoactivated. It can be envisaged that in the next future, the need for antiviral materials will attract more attention of carbon-based nanomaterials and new fields of applications can be expected to be developed.

2. Interaction of viruses and graphene

Application of graphene nanomaterials has been largely exploited in several fields, from electronics to sensing and photonics, but only to a minor extent in nanomedicine⁷. Graphene and graphene oxide have been used as anti-bacteria agents, drug or gene delivery⁸, cancer therapy⁹, engineering stem cell¹⁰, tissue engineering¹¹, biosensing¹² and bioimaging¹³.

In particular, graphene oxide has shown an antibacterial activity although a clear origin of such effect has not yet been identified^{14,15}. The antibacterial activity of graphene oxide (GO) and reduced graphene oxide (rGO) has been tested on E.coli bacteria. It has been



observed that GO produces damage to the membranes of bacterial cells, causing the exit of the cytoplasm. It has also been observed that E.coli cells respond to GO or rGO exposure in a different way. The E.coli cells are singularly wrapped by the GO layers, while in the case of rGO result embedded into large aggregates. GO show, in general, the highest antibacterial activity, which depends on time and concentration. The origin of this effect has been attributed to oxidative stress. In fact, GO and rGO oxidize the glutathione which acts as the redox state mediator in bacteria, and physically disrupting of the membrane via direct contact with the sharp parts of GO layers¹⁶.

2.1 Direct antiviral activity

The antibacterial activities of GO and rGO sheets suggested that these nanomaterials could also have a direct antiviral action. An evaluation of this activity has been performed using RNA (*porcine epidemic diarrhoea virus*, PEDV)¹⁷ and DNA (*pseudorabies virus*, PRV) viruses as a model¹⁸. PEDV is a coronavirus that infects pigs causing severe diarrhoea and dehydration, which result in significant mortality in piglets. PEDV cannot be transmitted to humans. PRV is, instead of a herpesvirus of swine, belonging to the *Alphaherpesvirinae* subfamily, which causes the Aujeszky's disease. Both the viruses are responsible for worldwide severe economic losses.¹⁹

In **Figure 1** is reported the antiviral effect of graphene oxide at noncytotoxic concentration. Experiments have shown that GO the inactivates the virus before it enters the cells. The virus has been inactivated by physical disruption of the structure through direct interaction with the sharp edge of the GO layers. Images taken by TEM have shown that the glycoprotein spikes in the virion envelop, after incubation with GO for one hour, have been destroyed. The antiviral activity was effective on both DNA and RNA viruses, and dependent on concentration and incubation time. Interestingly, it has been observed that rGO and GO showed a similar antiviral activity, which suggests a minor role of the surface functional groups. Because GO and rGO have a similar negative charge and layered structure, the physical interaction of the viruses with their sharp edges should be at the origin of the antiviral activity. GO has been found to inactivate the virus before they enter the cell. Another important factor is the negative charge of GO, which favours the electrostatic interaction with the positively charged viruses. The higher interactions result in the destruction and inactivation of the virus.

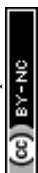
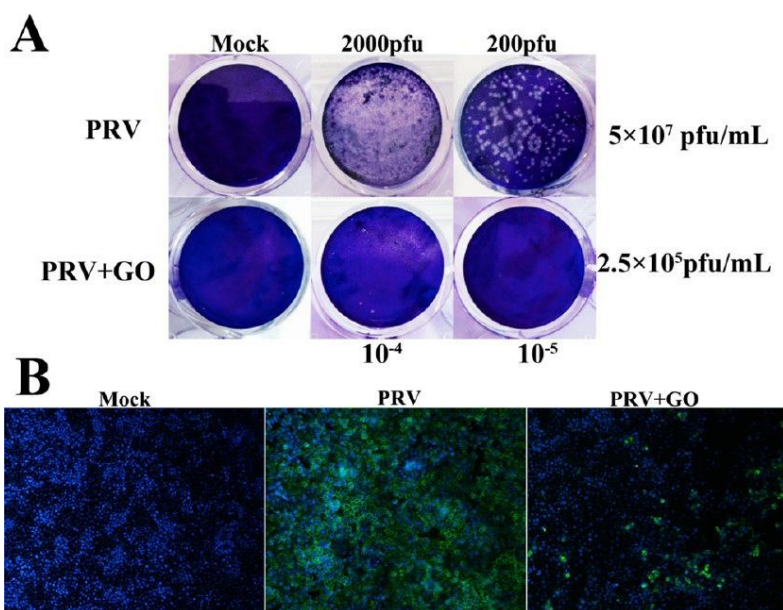


Figure 1. Anti-PRV activity of graphene oxide on PK-15 cells. (A) Plaque-reduction assay using PK-15 cells infected with PRV in the presence and absence of GO. The number of plaques (clear spots) job served represents the amount of virus in a given dilution. Mock infected cells (top left); cells infected with PVR of 2000 pfu (top middle) and 200 pfu (top right); cells treated with 6 $\mu\text{g}/\text{mL}$ GO (bottom left); PRV-infected cells in the presence of GO at 2000 pfu (bottom middle) and 200 pfu (bottom right). (B) Indirect immunofluorescence assay of PK-15 cells infected with PRV in the presence and absence of GO. Blue, DAPI; green, FITC-conjugated goat antimouse antibody. Reproduced with permission from ref.¹⁸. Copyright 2015 American Chemical Society.

A confirmation of GO negative charge role can be found in the experiments performed by Sametband et al.²⁰ They have tested the antiviral activity of GO layers and partially reduced sulfonated GO (rGO-SO₃). Both the nanomaterials have a negative charge, due to carbonyl and sulfonate surface groups, and can inhibit the infection from the herpes simplex virus type-1, HSV-1 (*Human Alphaherpesvirus 1*) (*vide infra*). HSV-1 is a double-stranded DNA virus, member of the Human Herpesviridinae family. It is an enveloped virus with a spherical pleomorphic structure whose diameter is around 200-250 nm. HSV-1 causes oral herpes or cold sores in a large portion of the world population. GO has been also tested as a label free nanomaterial to detect and inhibit the viral activity²¹. Two enteric viruses have been used, H9N2 (*endemic gastrointestinal avian influenza A virus*) and EV71, a virus responsible of hand, foot and mouth disease. H9N2 is a subtype of the *Influenza A virus* (bird flu) belonging to the *Orthomyxoviridae* family. EV71 is a non-enveloped virus of small dimension, about 30 nm in diameter, belonging to the *Picornaviridae* family. GO antiviral effect has been found to be strongly dependent on the temperature; at 25°C and 37°C only a weak antiviral activity has been detected, less than 0.5 and 1 log respectively. (**Figure 2**). Experiments have been performed in the presence of GO at 56°C, a threshold value for virus inactivation. In general, not all the viruses inactivate at 56°C, but when both the H9N2 and EV71 viruses lost their infectivity completely when GO is added.

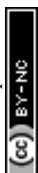
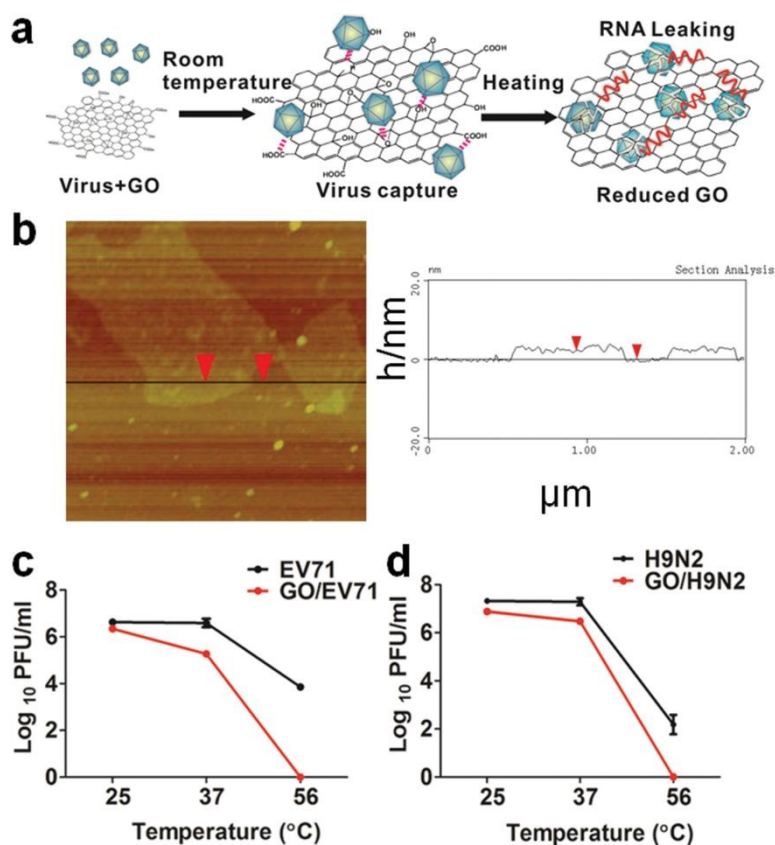


Figure 2. (a) Schematic representation of the GO and virus interaction exposed at different temperatures. The physiochemical interactions between viruses and reactive oxygenated groups were indicated by dotted lines. The release of viral RNA is described in red. (b) AFM images (left) and height profile (right) of the GO. (c) The temperature-dependent removal of EV71 and (d) H9N2 at room temperature (25 °C), physiological temperature (37 °C), and commonly used inactivation temperature of viruses (56 °C). Reproduced with permission from ref ²¹. Copyright 2014 WILEY-VCH Verlag GmbH & Co. KGaA, Weinheim.

The authors have underlined that the localized reactive oxygen groups on GO surface is a critical parameter to control the virus binding through the physicochemical reactions activated by the thermal reduction. The viruses captured by GO have shown a loss of structural integrity with destruction of the spike structures. Because of the virus integrity lost, an immediate leaking of RNA has been observed. This can be used as a process to extract RNA and a quick virus detection using one-step RT-PCR assay assisted by GO. After 30 min at 56°C, the content of leaked RNA in presence of GO was 46.9% for EV71 and 53% for H9N2 and only 5.6% and 6% without.

The direct effect produced by graphene sheets on Ebola virus has been also theoretically investigated. Molecular dynamic calculations have been used to simulate the interactions of graphene with Ebola VP40 oligomers²². The graphene layers are able to recognize and break the hydrophobic protein-protein interactions in the matrix protein VP40.

2.2 Antiviral activity through photocatalysis

Another way to inhibit the virus activity using GO is through photocatalysis. GO has a photocatalytic activity²³ which could be also exploited for inhibition of virus activity. To have a consistent photodegradation, the virus should stay close to the GO surface under UV irradiation. This type of strategy has been developed by Hu et al. to synthesise graphene oxide-aptamer nanosheets²⁴. The aptamers attached on the GO surface have been used to capture *MS2 bacteriophage viruses*²⁵. *MS2 bacteriophage* is a small (23-28 nm) icosahedral non-enveloped RNA virus, which infects the bacterium *Escherichia coli*. Because of its characteristic can be used as a model for testing the antiviral properties of GO upon illumination with UV light (**Figure 3**). In this case the breakage of the virus protein capsid is predominant with respect to the physical disruption produced by the sharp edge of the GO layers.



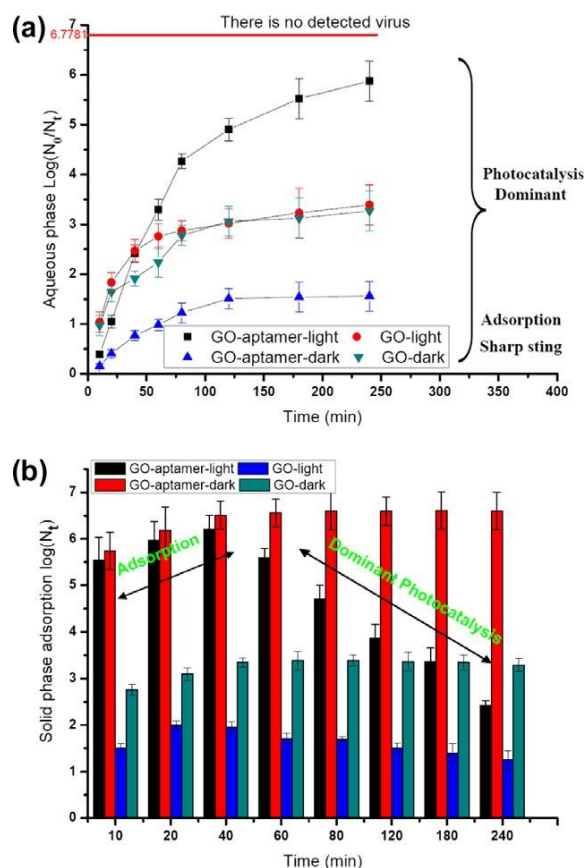


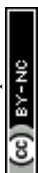
Figure 3. Survival viruses in aqueous phase (a) and solid phase (b) with visible-light irradiation or dark. The line of no detected viruses expresses only one virus in the suspension. Reproduced with permission from of ref²⁴. Copyright 2012 Elsevier Ltd.

In another example, GO layers have been used to produce a GO-Tungsten oxide composite whose antiviral activity has been tested under UV light irradiation using a MS2 bacteriophage virus on the surface of the material²⁶.

2.3 Graphene oxide – silver nanoparticle systems

Silver nanoparticles (AgNPs) have shown in different conditions a remarkable antiviral activity²⁷ and in combination with GO an enhanced antibacterial activity^{28,29}. The main mechanism of virus inhibition by AgNPs is the physical binding via the glycoprotein. The dimension of the particles is a crucial parameter since the size-dependent interactions with HIV-1 viruses have been found only in the 1-10 nm range. The AgNPs preferentially interact with the virus through binding to the glycoprotein. The virus bound to the nanoparticles are not able anymore to penetrate the cells.

This peculiar properties of AgNPs can be integrated with GO, which becomes a platform for the nanoparticles; this has the advantage of avoiding the agglomeration of the AgNPs while the negatively charged GO may attract the viruses. The therapeutic approach is based on using the NPs as an extracellular inhibitor avoiding the viruses to enter the cells. The antiviral activity of a GO-AgNPs nanocomposite has been tested with non-enveloped viruses, *feline coronavirus* (FCoV) and *infectious bursal disease virus* (IBDV)³⁰. The non-enveloped FCoV belongs to the family of *Coronaviridae* and species *Alphacoronavirus 1*. It infects cats worldwide and is responsible of the most common and deadly feline infectious diseases. IBDV is a double-stranded RNA non-enveloped virus of the *Birnaviridae* family and *Infectious Bursal disease species* with a diameter of 60-



65 nm. Only a limited antiviral activity has been detected; in the better case, the GO-Ag nanosystems have been able to inhibit 25% of infection by FCoV. View Article Online
DOI: 10.1039/D0SC02658A

A similar approach has been followed by Du et al., to prevent viral entry into the cells³¹. AgNPs have been self-assembled on the surface of GO via interfacial electrostatic forces. The inhibition efficiency was 59.2% in the case of porcine reproductive and respiratory syndrome viruses (PRRSV), which is an RNA virus with a strong impact on the pig industry (**Figure 4**). Interestingly, besides the antiviral effect due to the virus binding with the AgNPs, another mechanism has been suggested. The GO-AgNPs enhances the production of interferon- α (IFN- α) and IFN-stimulating genes (ISGs) which causes a direct inhibition of the virus proliferation.

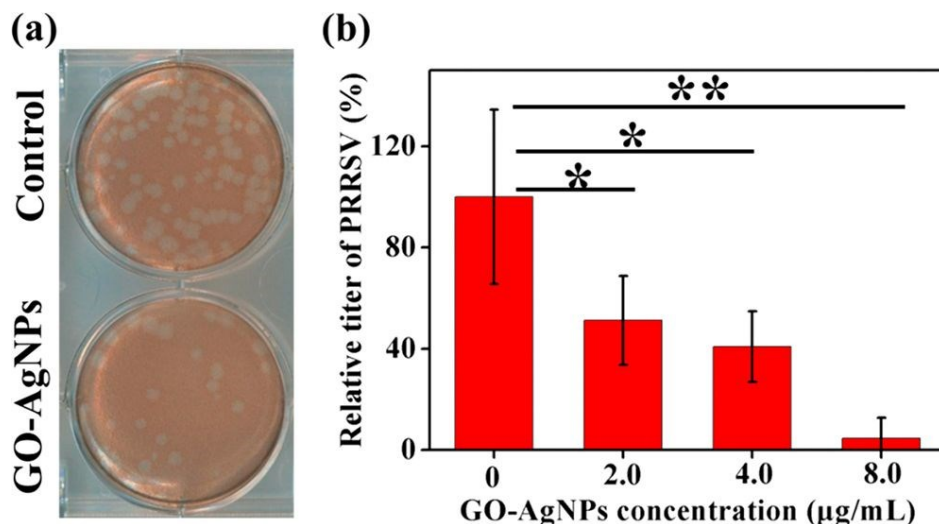


Figure 4. Effect of GO-AgNPs nanocomposites on the entry of PRRSV. (a) Plaque assays of the control and PRRSV pre-exposure with 4.0 µg/mL GO-AgNPs nanocomposites. (b) The influence of concentrations of GO-AgNPs nanocomposites on the relative titer of virus. Reproduced with permission from ref. ³¹. Copyright 2018 American Chemical Society.

2.4 Mimicking the cell surface

Another extracellular route to inhibit the virus activity is using GO layers as a platform to mimic the cell surface receptors. GO derivatives, obtained by binding on the nanosheet surface heparan sulphate (HS), have shown to compete with HSV-1²⁰. HS is a linear polysaccharide which is negatively charged. HSs are attached to the cell surface as proteoglycan (HPG) and may become cellular receptors for different viruses. To mimic the surface of the cell, GO layers have been functionalized by sulfonated groups (GO-SO₃), as previously discussed²⁰.

Other examples to mimic the extracellular cell matrix have been reported, which include GO functionalization with polyglycerol sulfate³², β -cyclodextrin³³ and polyglycerol sulphate in combination with alkyl chains³⁴.

A main issue regarding the functionalization of GO is controlling the density and distribution of the groups attached to the surface. Gholami et al³⁵, have developed a one-pot [2+1] nitrene cycloaddition reaction to functionalize graphene by 2-azido-4,6-dichloro-1,3,5-triazine (**Figure 5**). In a second step, the GO surface has been covered with sulphonate groups using polyglycerol with few amino functional groups PG(NH₂)₄%. This method has allowed obtaining a platform with a uniform distribution of hyperbranched polyglycerol on the surface. In a further step, the surface has been sulphated to obtain a



heparin sulphate mimetic 2D material. The nano-platform is highly negative surface charged and has a very good dispersibility in an aqueous environment. The capability of this platform to bind viruses has been tested using *Vesicular Stomatitis Virus* (VSV) as a model. VSV is an enveloped virus belonging to the *Rhabdoviridae* family and *Indiana vesicolorum* species. It is a zoonotic virus which is commonly used for laboratory studies of viral evolution in *Rhabdoviridae* viruses.

GO layers with only hydroxyl groups have shown a small affinity towards VSV in comparison with the GO with a high density of sulphates. In physiological conditions, the sulphate groups have been considered the main cause of the interaction between GO and the viruses in physiological conditions. The virions do not show any change after binding to the sulphonated GO platform. The authors have, therefore, excluded any disinfection activity on VSV from the action of the reactive oxygens generated by GO¹⁶. A GO-based 2D platform composed of 6% graphene and 94% sulphated polyglycerol has found to be able trapping 20 virions.

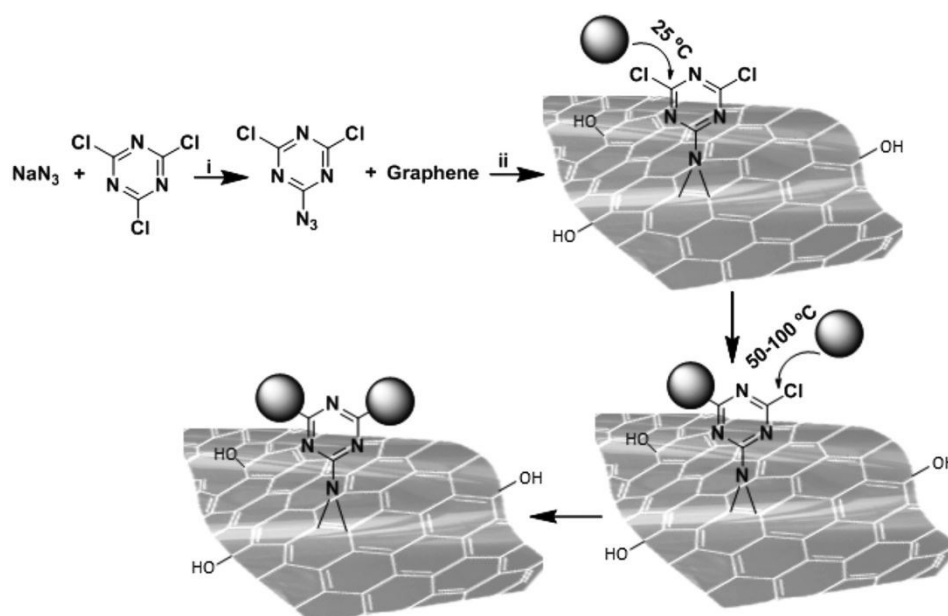
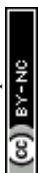


Figure 5. Functionalization of graphene by [2+1] nitrene cycloaddition using 2-azido,4,6-dichloro-1,3,5-triazine as nitrene precursor. Stepwise nucleophilic substitution of chlorine atoms of triazine groups at different temperatures resulted in controlled post-functionalization of thermally reduced graphene oxide-triazine. Reaction conditions; i = N-methyl-2-pyrrolidon, 0 °C, 1 h and ii = Sonication, stirring, room temperature 70 °C, 24 h. Reproduced with permission from ref.³⁵. Copyright 2017 WILEY-VCH Verlag GmbH & Co. KGaA, Weinheim.

A very similar strategy has been developed by Ziem et al.³², to create a mimetic extracellular matrix via functionalization of graphene sheets with polyglycerol sulphates. The entry inhibition has been evaluated using two enveloped viruses with a double stranded DNA genome, *Pseudorabies Virus* (PrV, Suid herpesvirus 1) and *African swine fever virus* (ASFV). ASFV is an enveloped icosahedral, double stranded DNA virus of large dimensions (170-190 nm diameter). ASFV causes the *African swine disease* which is deadly for pigs.

The surface has been functionalized using linear or dendritic polyglycerol sulphate which give negatively charged GO platforms (**Figure 6**). The linear polyglycerol azides have a higher inhibitory effect in comparison to the dendritic one in the case of PrV but the effect is analogous for ASFV. The linear conformation favours the interaction with the virus because is more like the heparan sulphate in the extracellular matrix which interacts with the herpes viral glycoproteins gB and gC.



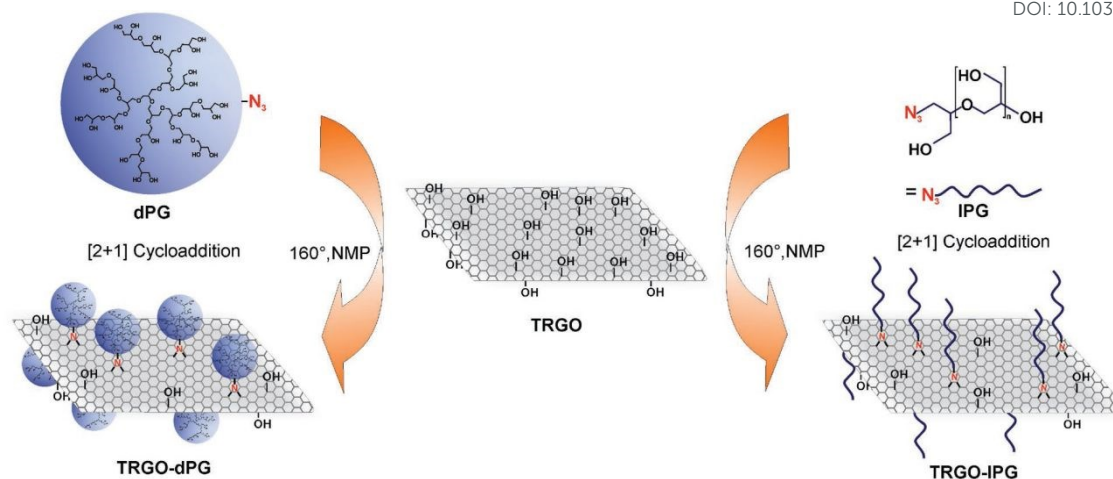


Figure 6. Schematic representation of the inhibitor development by combining thermally reduced graphene oxide (TRGO) with either dendritic polyglycerol (dPG) azide or linear polyglycerol (IPG) azide. Reproduced with permission from ref.³². Copyright 2017 WILEY-VCH Verlag GmbH & Co. KGaA, Weinheim.

Another graphene platform to bind viruses has been developed by Donskyi et al. who functionalized GO by polyglycerol sulphate and fatty amine functionalities³⁴. The interaction of such platform with *Herpes Simplex Virus type 1* (HSV-1) has been studied. The combination of sulphate and alkyl chains produces binding of the virus through the electrostatic interactions with the polyglycerol sulphate while the alkyls induce a high antiviral activity by secondary hydrophobic interactions. Alkyl chains of different lengths (C₃–C₁₈) have been tested. Longer alkyl chains have been found to have the highest antiviral activity, but they are also toxic against Vero cells. The best compromise in terms of toxicity and antiviral effects is observed in layers functionalized with C₆ and C₉ alkyl chains.

GO has been also used as a platform for curcumin, a natural polyphenol, which is known for its antioxidant, antibacterial and antiviral activity³³. Curcumin was efficiently linked to the GO surface via β -cyclodextrin molecules used as intermediate sites (**Figure 7**). The antiviral effect of the system has been tested with *Respiratory Syncytial Viruses* (RSV). RSV is an enveloped RNA virus (120 – 200 nm in diameter), belonging to the *Pneumoviridae* family and *Human Orthopneumovirus* species.

The antiviral activity of the nano system has been explained on the base of three different mechanisms that could synergistically operate, inhibition of the virus attachment on the surface of the cells, interference of the virus replication and direct inactivation of the virus.



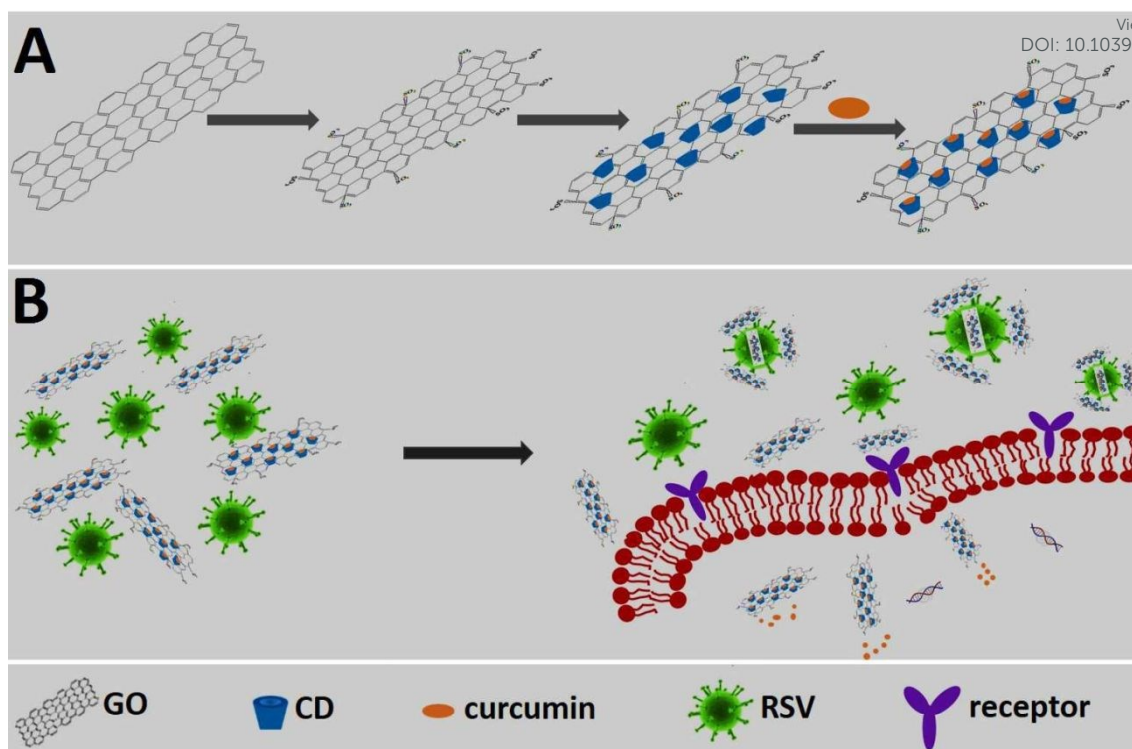


Figure 7. Schematic representation of work principle. (A) The synthesis of functional nanomaterials composite; (B) The proposed inhibition mode of functional nanomaterials composite against RSV infection. Reproduced with permission from ref. ³³. Copyright 2017 The Royal Society of Chemistry.

Controlling the graphene-virus interactions, which could be direct or mediated through surface functionalization, depends on several parameters. In particular, the dimension, the number of layers, the surface wrinkling and the geometrical topology of the layers have a key role. The interaction of graphene with three key target proteins, HIV-Vpr, Nef and Gag, of HIV has been modelled to evaluate the effect of the number and size of layers³⁶. The bonding affinity of graphene does not increase with numbers of layers, from 1 to 5 layers no changes should be expected on the base of the theoretical calculations. On the other hand, increasing the size produces an enhancement of the binding affinity.

2.5 Platform for antiviral drugs

The possibility of using GO as a platform has been, as we have seen, exploited to produce nanosystems with the capability of binding the viruses, producing an extracellular matrix which blocks the virus before they can attach to the surface of the cell. Another possibility is using GO as a 2D platform to load drug with a recognized antiviral activity. Hypericin (HY) is an anthrone derivative which is largely used as antiviral for several retrovirus, such as HSV-1, Sendai virus and duck hepatitis B. HY has been loaded on GO via physisorption, through the π - π stacking and hydrophobic interactions³⁷. The advantage of this approach is that HY is slowly released and this decreases its cytotoxic effect. The GO-HY system has shown an effective capability to inhibit viral replication using novel duck retrovirus as a model.

2.6 Search and destroy strategy



Functionalization of graphene oxide surface with sulphonate groups allow binding the viruses and avoiding or limiting the interactions with the cells³⁸. This strategy has been improved by anchoring on the graphene surface (**Figure 8**). After the viruses have been captured by the graphene layers, they can be removed using the magnetic nanoparticles and finally inactivated by exposure to near infrared radiation.

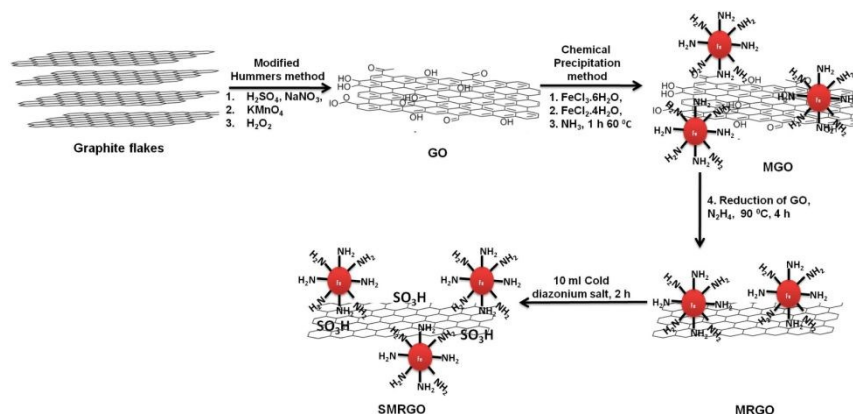


Figure 8. First, graphite was oxidized to GO by a modification of Hummer's method. Next, the GO was functionalized with magnetic nanoparticles and reduced to MRGO. Last, the MRGO was sulfonated to yield SMRGO. Reproduced with permission of ref. ³⁸. Copyright 2017 American Chemical Society.

The high thermal conductivity of graphene is correlated to its excellent capability of light-to-heat conversion. This property has been used for photothermal³⁹ and photodynamic⁴⁰ treatments of cancer cells and bacteria. The sulphonated reduced graphene oxide with grafted magnetic iron nanoparticles has shown a remarkable capability to inactivate HSV-1. 99.99% of the virus have been inactivated within 10 minutes upon irradiation with NIR light.

3. Antiviral Effects of Carbon dots

So far, we have seen that 2D materials, in this case graphene and graphene oxide, exhibit interesting antibacterial and antiviral properties and have relevant characteristics as functionalized platforms against viruses of various kinds. It is worth considering another family of carbon based nanomaterials, which has attracted great attention in recent years for their excellent optical properties and ease of synthesis, the carbon dots (C-dots).^{41–43} Studies on the antiviral properties of carbon dots are very recent and in small numbers. Nevertheless, they show promising opportunities for such nanomaterials.

Carbonization of organic precursors can give carbon-based nanoparticles, whose structural characteristics, although still debated, can be easily engineered thanks to an appropriate choice of precursors.^{44–46} More precisely, C-dots represent a large family of carbon-based materials, whose structure is still under debate. Different type of nanomaterials are included in the family of C-dots, amorphous carbon nanoparticles, partially graphitized core-shell carbon nanoparticles, amorphous fluorescent polymeric nanoparticles and graphene quantum dots (GQD). GQD are small fragments of graphene, with a lateral size < 10 nm and share many properties with carbon dots and graphene. The large variety of C-dots results in potential applications ranging from photocatalysis to bioimaging. However, in addition to the remarkable optical properties that make them the main candidates for new generations of optoelectronic devices, C-dots have also shown an active role against infections. This is mainly due to the functional groups on the surface, which in turn are responsible for their extraordinary optical properties. As we



will see, these functional groups influence the antiviral properties of C-dots, making them active against a virus or even determining their broad-spectrum effects.

Recent experiments have shown that some nanostructures functionalized with boronic acid are able to inhibit the entry of some viruses and block their attachment⁴⁷. In the light of these results, C-dots made from boronic acid precursors have been recently particularly relevant. C-dots have been tested against *Herpes simplex Virus Type 1* (HSV-1) with encouraging results. The experiments were performed under classical in vitro conditions on monkey kidney cancer cells (Vero) and human lung cancer cells (A549) and cytotoxicity and antiviral assays were performed. The properties and functionality of three different types of C-dots, made with hydrothermal technique, have been investigated. The precursors of C-dots have guaranteed the formation of different functional groups, revealed through vibrational spectroscopy techniques. Phenylboronic acid (PBA), 3-aminophenylboronic acid (3-APBA), or 4-aminophenylboronic acid hydrochloride (4-APBA) have been used as precursors. After treatment at 160 °C for 8 h the products have been dialyzed before being used for in vitro study.

The cytotoxicity study has revealed that all three C-dots were non-cytotoxic on A549 at concentrations of up to 300 $\mu\text{g mL}^{-1}$. Moreover, PBA and 4-APBA derived C-dots showed no cytotoxicity to Vero cells, although 3-APBA based C-dots were moderately cytotoxic. As shown in **Figure 9**, at a concentration higher than 5 $\mu\text{g mL}^{-1}$ of 3-APBA/C-dots and 4-APBA/C-dots, no infection has been detected with a 100 % cell viability. On the contrary, PBA/C-dots have shown no effectiveness against virus infection. Interestingly, the results of C-dots role can be revealed by a morphological study of cell. As a result of virus presence, the cells undergo an important change in shape and dimensions, while being unaltered under a treatment with C-dots. The contrast mechanism of C-dots to the virus is not completely understood. Indeed, it has been confirmed that boronic acid is not involved in the inhibition of HSV-1, in contrast to other boronic acid modified nanostructures. C-dots have a significant impact at the early stage of virus entry by interacting more with Vero cells than with viral entities, interfering in the interaction between cell receptors and virus⁴⁸.

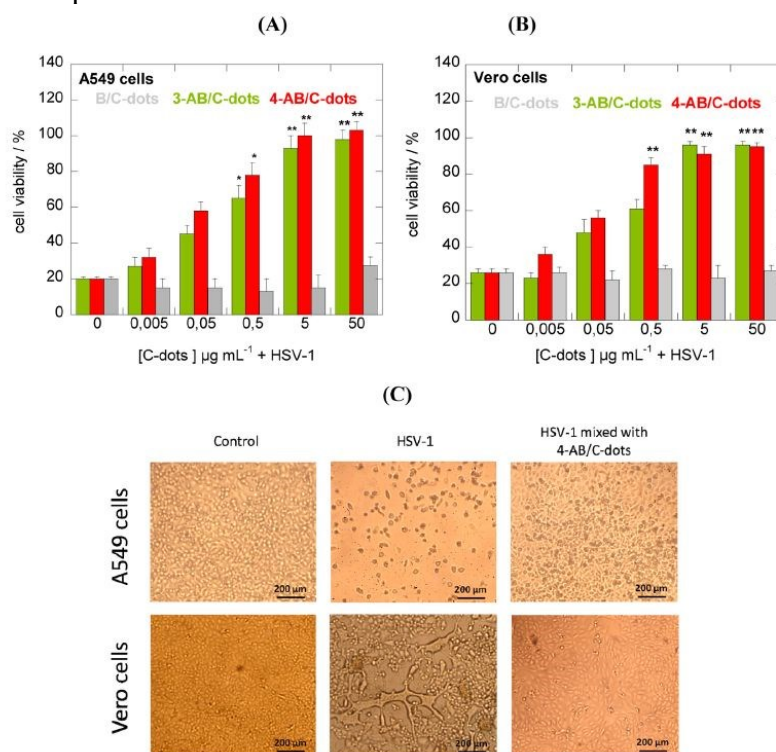


Figure 9. C-dots inhibition effects of HSV-1 on A549 (A) and Vero (B) cells at different concentrations (C) Morphological effects of C-dots treatments. Reproduced with permission from ref. ⁴⁸. Copyright 2016 American Chemical Society.

The effect of virus inhibition of C-dots has been also tested with *Human Immunodeficiency Virus HIV-1* infections. HIV-1 is the *Retrovirida* family virus, with a diameter of 120-200 nm which is responsible of the disease.

C-dots with a hydrodynamic diameter of about 3 nm have been prepared by carbonization of citric acid anhydrous at 200 °C for 30 min and dialyzed thereafter. The obtained C-dots have been also functionalized with 4-carboxy-3- chlorobenzeneboronic acid (CBBA/C-dots). In this case, the role of boronic acid groups has been pointed out. C-dots and CBBA/C-dots have been mixed with MOLT-4 cells to assess the cytotoxicity. Both dots have appeared safe, up to a high concentration of 300 $\mu\text{g mL}^{-1}$, with cell viability over 80 % even at 300 $\mu\text{g mL}^{-1}$. The corresponding CC_{50} values were 2901.2 and 1991.9 $\mu\text{g mL}^{-1}$. The antiviral role of C-dots and CBBA/C-dots has been studied by evaluating syncytia formation. Indeed, one of the most efficient ways of virus transitions from an infected cell to normal cell takes place with direct contact. Counting the numbers of syncytia in the presence of dots can be a good manner of evaluating the virus infection. As a result, C-dots have not prevented the formation of syncytia, while CBBA/C-dots have bonded to gp120 on the virus, blocking the infection by preventing the MOLT-4 cells from binding (**figure 10**). Although hydroxyl and carboxylate surface groups on C-dots can contrast HIV infection, by the formation of hydrogen bonding with the molecules of the viral envelope, the boronic acid tends to enhance this effect, by interacting with 1,2-cis diols sites on gp120.⁴⁹

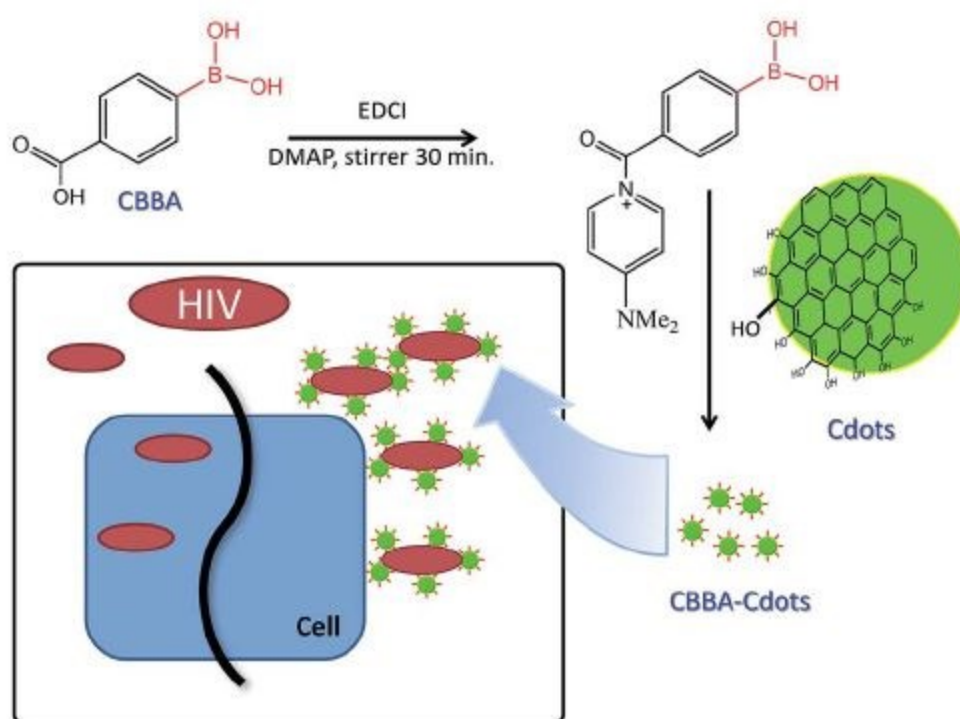
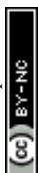


Figure 10: proposed mechanism of CBBA/C-dots on the inhibition entry of HIV-1. Reproduced with permission from ref. ⁴⁹. Copyright 2016 The Royal Society of Chemistry.

PEG-diamine and ascorbic acid derivate C-dots have shown encouraging results as viral inhibitors by active functionality. The dots, showing a low level of cytotoxicity with cell viability of 72 % after 48 h incubation at the concentration of 0.250 mg mL^{-1} , have been



tested on Monkey kidney (MARC-145) and Porcine kidney (PK-15). In particular, MARC-145 cells have been infected by porcine reproductive and respiratory syndrome virus (PRRSV) and PK-15 by *Pseudorabies Virus* (PRV). Virus titers have been reduced in presence of C-dots in comparison with the control groups (**Figure 11**). PRV has been also studied by indirect immunofluorescence assay of PRV-gD and PRV-VP16, as responsible for binding with host cell receptors and a component of primary enveloped virions, respectively. The samples treated with C-dots have shown a significant decrease of fluorescence in accordance with titer count. The experiments on PRRSV have had the same conclusions, with remarkable inhibitory effects of CDs. At the same time, the investigation of type I interferons (IFNs) α , antiviral innate immune molecules, and the IFN-stimulated genes (IFGs) have indicated a possible inhibitory mechanism of C-dots to the activation of IFN- α and production of ISGs.⁵⁰

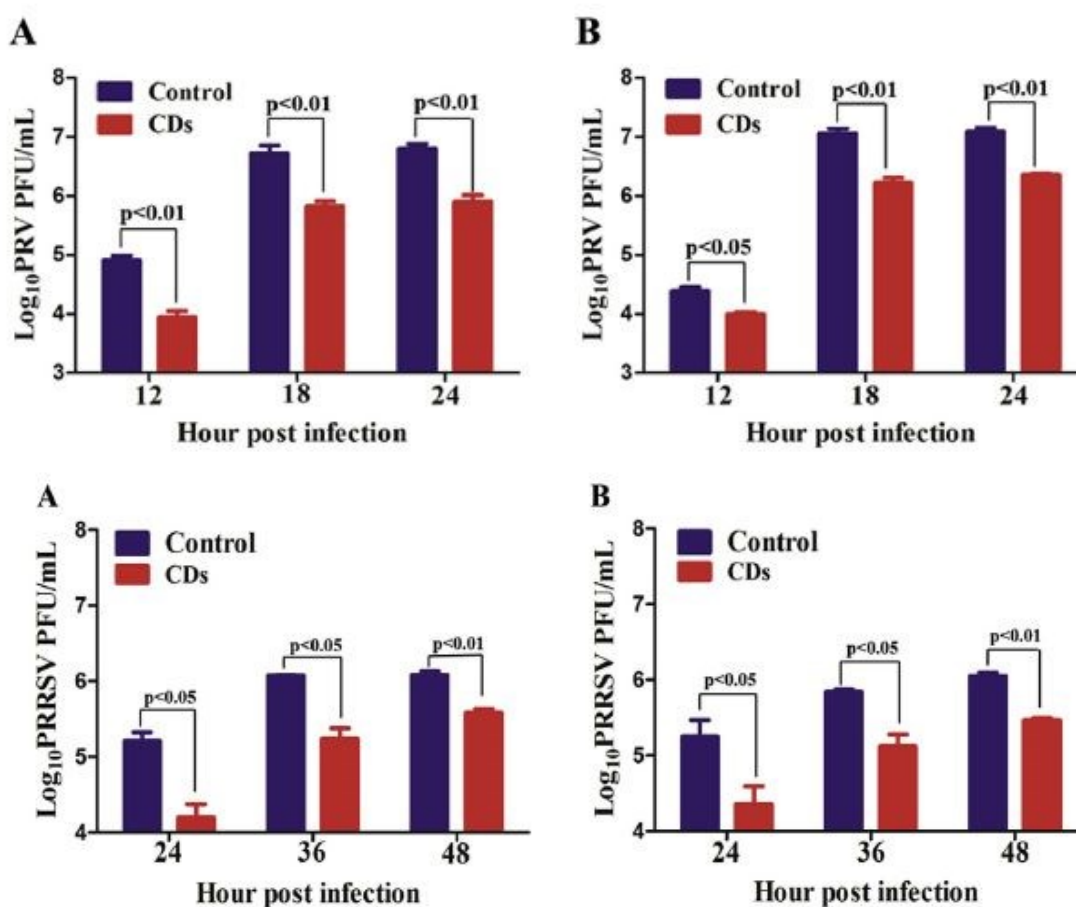


Figure 11: replication process of PRV (top) and PRRSV (down). Reproduced with permission from ref.⁵⁰. Copyright 2016 Elsevier Ltd.

Similar results have been obtained for curcumin derived C-dots, exploiting the antiviral activity of herbs^{51,52}. They have been applied to porcine epidemic diarrhoea virus (PEDV) as a coronavirus model. Ting et al. have treated a mixture of citric acid and curcumin at 180 °C for 1h under hydrothermal conditions (CCM/C-dots) and confronted them with more common ethylenediamine based dots (EDA/C-dots). It has turned up that CCM/C-dots display a great efficacy against the replications of PEDV in comparison with EDA/C-dots. In fact, CCM/C-dots can act modifying the structure of the surface protein in viruses, suppressing negative-strand RNA of virus and the accumulation of reactive oxygen species and stimulate the production of ISGs and cytokines. The inhibition of PEDV in Vero cells at the CCM/C-dots concentration of 125 $\mu\text{g mL}^{-1}$, has been studied by titers



counts and green fluorescence signal of PEDV N proteins. The CCM/C-dots present a positive charge that strongly interacts with PEDV and the cell membranes and competes with the virus to bind to the cell surface. The z-potentials of CCM-CDs, PEDV and CCM-CDs pre-treated with PEDV resulted in +15.6, -6.42 and -0.18 mV, respectively. Thereby, the positive potential of C-dots can promote the aggregation of virus and reduce the infectivity, as verified by fluorescence and Raman measurements⁵².

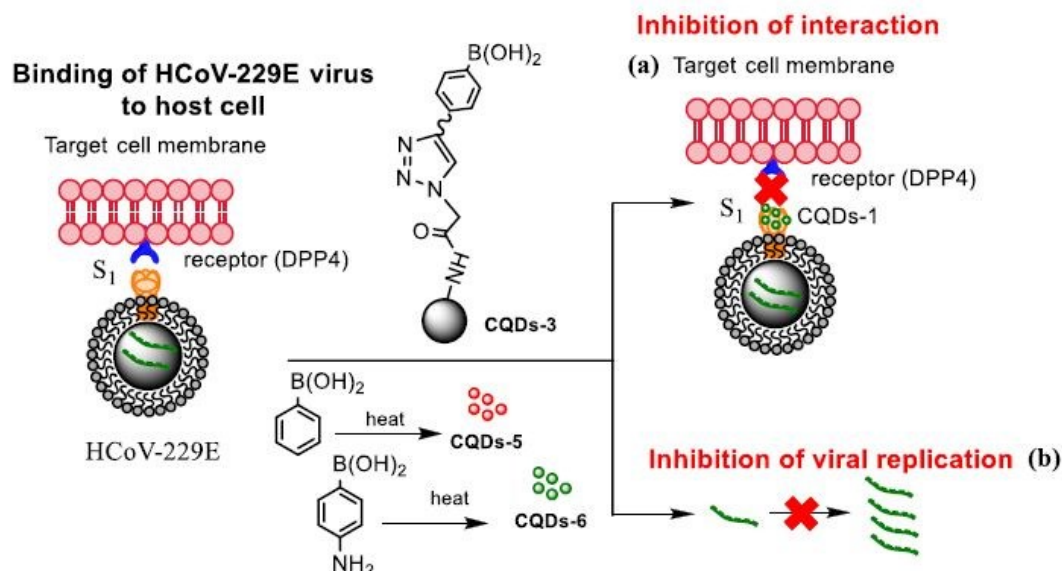


Figure 12: Scheme of carbon dots inhibition mechanism of HCoV-229E. Reproduced with permission from ref. ⁵³. Copyright 2019 American Chemical Society.

Although the mechanism of action of carbon dots is still far from being fully understood, it has been well established that the role of functional groups deriving from the appropriate choice of different precursors is a fundamental parameter. This is what emerges from the experiments of Łoczechin et al.⁵³, where different C-dots have been tested as a countermeasure to the proliferation of *HCoV-229E* Human Coronavirus in Huh-7 cells. HCoV-229E is an enveloped, single-stranded RNA coronavirus. It is one of the viruses which cause the common cold with a 120-160 nm diameter. (*Coronaviridae* family, *Human coronavirus 229E* species). As in previous works, the primary role of C-dots is to act at the early stages of infection, inhibiting the interaction of the S-receptor protein with the host cell membrane (**Figure 12**). However, not all C-dots have shown the same effectiveness, underlining the importance of molecular groups resulting from synthesis. In this work, a first group of C-dots have been synthesized by hydrothermal carbonization of ethylenediamine/citric acid and functionalized according to the scheme of **Figure 13**.

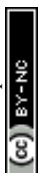
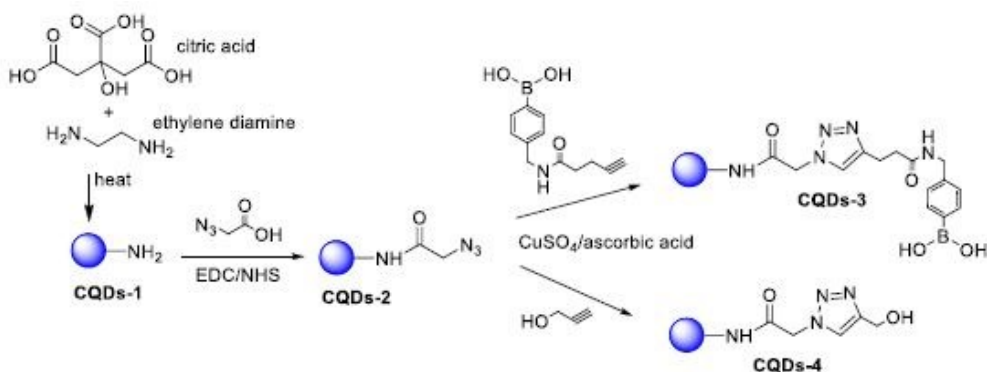


Figure 13: scheme of functionalization of EDA/citric acid derived C-dots. Reprinted with permission from ref. ⁵³. Copyright 2019 American Chemical Society. View Article Online
DOI: 10.1039/D0SC02658A

In general, the highest efficacy of C-dots occurs in the first period after infection, at about 1 h after inoculation. However, they have shown significant inhibition activity even after 5.5 h. Still, the mechanism of inhibition must be figured out although it seems to be based on the interaction with cells.

Lin et al.⁵¹ have suggested that the C-dots can act at different levels of infections. Again, curcumin derived C-dots have been realized by pyrolyzing curcumin at different temperatures. C-dots have been tested against EV71 virus in RD cells. C-dots can hinder the interaction of the virus with RD cell membranes. Contemporary, they can suppress the ROS (Reactive oxygen species) working as radical scavengers and inhibit PGE₂ production. Furthermore, it has also been reported that curcumin C-dots can decrease the expression of p38 kinase.⁵⁰

A further step forward is represented by C-dots from benzoxazine. Contrary to the previous examples, where an important role of boronic acid was highlighted, in this case the effectiveness of boron-free C-dots has been demonstrated. In addition to the well-known biocompatibility, these hydrothermal synthesised C-dots made from the monomer benzoaxine BZM have demonstrated a broad spectrum efficacy in blocking virus infectivity. Unlike other systems, where multiple mechanisms can intervene in antiviral activity, in this case the C-dots have shown a direct interaction with virions. C-dots have been employed against flaviviral (JEV) infections on BHK-21 cells⁵⁴. To investigate the broad-spectrum potentialities of C-dots, different viruses have been treated, both enveloped and non-enveloped. Although the dots present a marked effect on JEV and ZIKV, they have demonstrated suitable for other viruses. The EC₅₀ of BZM/C-dots against different viruses is 18.63 μg mL⁻¹ (JEV), 3.715 μg mL⁻¹ (ZIKV), 37.49 μg mL⁻¹ (DENV), 40.25 μg mL⁻¹ (AAV), and 45.51 μg mL⁻¹ (PPV)⁵⁴.

Finally, it is worth to mention that carbon nanoparticles with 2,2'-(ethylenedioxy)bis(ethylamine) and 3-ethoxypropylamine have been proved to inhibit the human norovirus virus-like-particles (VLPs) interaction with HBGA receptors, leaving intact the morphology of VLP particles⁵⁵. Additionally, VLPs have been hampered in interacting with their respective antibodies.

Unlike the other carbon materials within the C-dots classification, whose optical properties are mainly governed by the presence of fluorophores or functional groups produced during the synthesis, GQDs photoluminescence originates from quantum confinement effects, related to their size. Thus, the fluorescence emission can be tuned through the size of graphene monolayers. GQDs can be obtained by thermal oxidation of graphene oxide, where epoxy and hydroxyl groups operate as cleavage sites and promote the GO cutting into smaller fragments^{56,57}. Mixtures of acids, e.g. nitric and sulphuric, are often employed for oxidative cleavage of graphitized carbon-based materials, although there are non-acidic alternatives such as oxone and H₂O₂. In addition, the electrochemical cutting of graphene, graphite, coal and so on, and ultrasonic exfoliation allow for high yield GQDs production^{58,59}. GQDs have attracted a lot of attention because of their extraordinary potential in the biomedical field. In particular, they have proven to be efficient and biocompatible emitters⁶⁰, which can be used for the detection of *Hepatitis C Virus* core antigen⁶¹, *hepatitis B virus*⁶² and cancer-targeted fluorescent imaging⁶³. GQDs have shown remarkable antiviral activity against HIV-1 infections. The most important experimental evidence of this efficacy has been reported by Iannazzo et al.⁶⁴ and remains the most significant so far. In their work, GQDs have been synthesized by acid oxidation and exfoliation of multiwalled carbon nanotubes. The activity of pristine dots have been



compared with the antiretroviral agents CHI499 and CDF119. Furthermore, QDs have been conjugated with CHI499 and CDF119 as drug delivery systems. The systems have been tested as inhibitors of HIV in cellular and enzyme assays, whilst the cytotoxicity has been studied in MT-4 cells. QDs have shown antiviral activity with an IC_{50} of $37.6 \mu\text{g mL}^{-1}$, an EC_{50} value in cell of $19.9 \mu\text{g mL}^{-1}$. Among the different candidates, QD/CHI499 system displays the most encouraging results. Indeed, the conjugated platform has shown improved antiviral properties, with an IC_{50} of $0.09 \mu\text{g mL}^{-1}$ and an EC_{50} of $0.066 \mu\text{g mL}^{-1}$ and selectivity index of 362. Accordingly, it has been supposed that the efficacy as drug deliver relies on the imide bond in QD/CHI499. After drug release in the infected cell, both QD and CHI499 can synergistically act as inhibitors. On the contrary, the amide bond in QD/ CDF119 prevents an easy drug release⁶⁴. Although the results open new opportunities of application as antiviral, QDs have displayed a more significant potential in bioimaging and sensing^{58,65}.

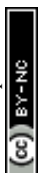
4. Fullerenes as antivirals

Fullerenes and its derivatives are the first class of carbon-based nanostructures to have been discovered (1985) and their chemistry and properties have been the subject of an extensive investigation. Potential biological applications in several fields have been developed using specific fullerene derivatives⁶⁶. Fullerenes have been also the first carbon compound to have been tested, in comparison to graphene and C-dots, as antiviral.

4.1 Fullerenes as anti-HIV agents

The first report about the antiviral activity of fullerenes is dating back to 1993⁶⁷. It was recognized that fullerene derivatives have an anti-HIV activity by blocking its encoded enzymes because the bulky fullerenes fit well into the active sites of HIV protease. A diamido diacid diphenyl fulleroid derivative was specifically designed to inhibit an HIV enzyme. Since then several research groups have worked on tailoring the synthesis of fullerene derivatives to inhibit the activity of HIV enzymes, HIV-1 RT and DNA polymerase. The general strategy is the same, developing a fullerene derivative able to inhibit the HIV enzymes. Different antiviral effects have been observed depending on the fullerene functionalization⁶⁸⁻⁷⁷. A comparative table with the main results can be found in ref. ⁷⁸. The main problem is balancing the cytotoxicity with the antiviral activity. In general, low cytotoxic effects have been observed for fullerene derivatives but the data still need more experiments to fully address some critical points, such as the presence and the effects of C_{60} derivative isomers.

The low solubility of fullerenes in water represents a strong limitation for their applications in biology⁷⁹. The preparation of soluble derivatives is, therefore, a mandatory step. An example of antiviral application of highly water-soluble fullerene derivatives has been shown by Troshima et al. in 2007 ⁸⁰. Using chlorofullerene, $C_{60}Cl_6$, as precursor substrate, polycarboxylic fullerenes in high yield have been obtained. The fullerene derivatives in the form of alkali metal salts have a high solubility in water ($50-100 \text{ mg mL}^{-1}$ at $\text{pH} < 7.5$) and a significant anti-HIV activity with a low cytotoxicity. Another question to be addressed is the potential antiviral activity by water soluble derivatives of fullerenes with larger carbon cages, such C_{70} . In comparison to C_{60} , because of the lower symmetry, synthesis of C_{70} water soluble derivatives is more difficult. Kornev et al. have prepared highly soluble C_{70} compounds whose antiviral activity and cytotoxicity has been tested⁸¹. A significant antiviral activity against HIV and influenza virus, H1N1 and H3N3, has been detected. *Influenza A virus* subtype H1N1 is a subtype of influenza A virus, belonging to the *Orthomyxoviridae* family (80 – 120 nm in diameter). H3N3 is another type of *Avian influenza virus* of the same family. Interestingly, a new antiviral



mechanism, through the interaction of the C_{70} derivatives with the envelope gp120 protein from HIV-1(III_B), has been observed. This protein is used by the virus to enter the cells via specific surface receptors recognition.

Besides HIV the inhibition of viral activity by fullerene derivatives has been tested for hepatitis C virus (HCV)⁸², respiratory syncytial virus (RSV)⁸³, virus H1N1, herpes simplex virus⁸⁴, human cytomegalovirus⁸⁴, Zika and Dengue viruses⁸⁵.

4.2 Antiviral activity of non-derivatized fullerenes

An interesting question raises: is pristine C_{60} capable of any direct effect on the viruses? Non-derivatized C_{60} has been found to inhibit the replication of simian immunodeficiency virus (SIV) and the activity of *Moloney Murine Leukemia virus* (M-MuLV) reverse transcriptase⁷⁷. 50% inhibitory concentration (EC₅₀) of non-derivatized C_{60} was 3 μ M but explanation of the mechanism has not been reported.

4.3 Viral inactivation via photosensitized production of singlet oxygen by C_{60}

An important property of fullerene is the capability of generating singlet oxygen (1O_2) with a high quantum yield, 0.96, upon illumination in the visible region (535 nm)⁸⁶. The generation of singlet oxygen^{87,88} by fullerenes has been used for antimicrobial⁸⁹ applications and for removal of pollutants⁹⁰. Singlet oxygen as oxidant agent in comparison to hydroxyl radicals ($\cdot OH$) is characterized by a longer lifetime (τ), 2-4 μ s with respect to 1 ns of $\cdot OH$. Hydroxyl radicals are also non-selective oxidants while singlet oxygen, which has a low reduction potential is more specific. Several research groups have explored the possibilities of using photoactivated fullerenes and some of its derivatives as antiviral agents.

A first set of experiments has been dedicated to investigating the photodynamic inactivation of enveloped virus by suspensions of non-derivatized C_{60} . Based on the known effect of singlet oxygen on virus inactivation⁹¹, C_{60} suspensions have been used as inactivating agents. The low solubility of fullerenes, in this case, is a positive property because allows, in principle, an easier and complete removal of the photosensitizer from aqueous solutions^{92,93,94}. Other sensitizers, such as hypericin if remain in biological fluids can be potentially toxic. An aqueous fullerene suspension has been used as photosensitizer to inactivate an enveloped virus, H1N1, in an allantoic fluid of chicken embryos⁹⁵. Damage of the surface membrane and a loss of surface glycoproteins has been observed upon irradiation of at least 2 hours.

Four different photosensitized aqueous fullerene suspensions have been used to inactivate the *MS2 bacteriophage*⁹⁶. The (1O_2) generation rate follow the order: $C_{60}(NH_2)_6 > C_{60}(OH)_{24} \approx aqu-nC_{60} > C_{60}(OH)_6$. The singlet oxygen produced an alteration of the capsid protein secondary structures and protein oxidation. MS2 inactivation appears to be the result of the loss of capsid structural integrity and the reduced ability to eject genomic RNA into its bacterial host have been considered the causes of MS2 inactivation (**Figure 14**).

The main application of fullerene suspensions which has been envisaged is to prevent the transmission of viral infections via plasma⁹⁷. Using C_{60} as photosensitizer has shown to allow a full inactivation of enveloped viruses in irradiated plasma.



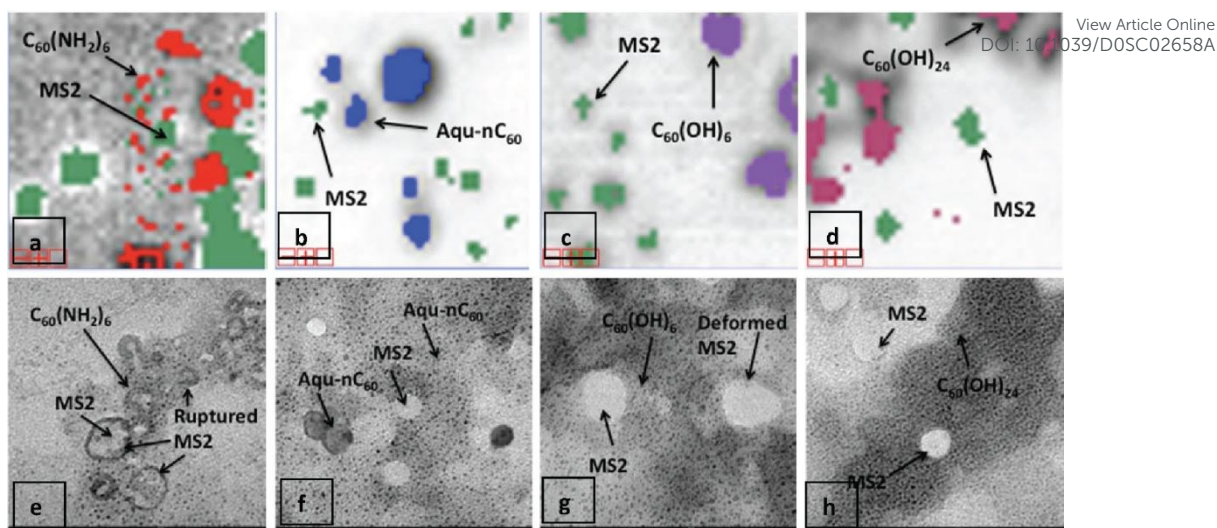
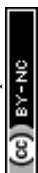


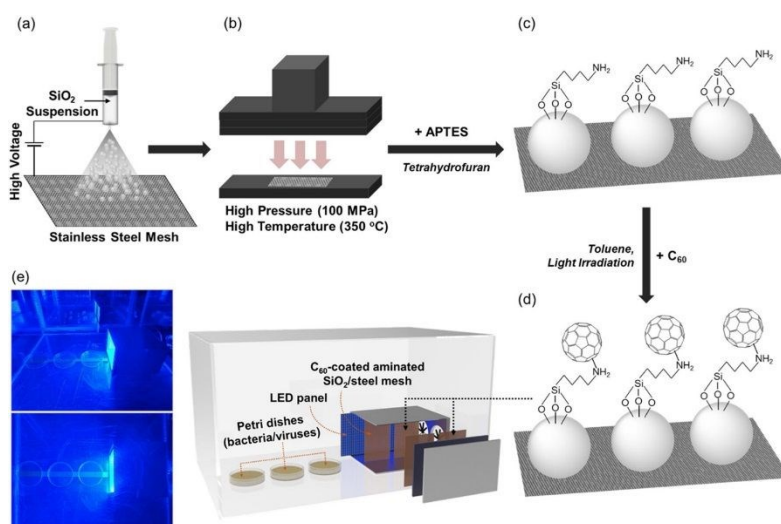
Figure 14. Relative proximity of various fullerenes with MS2 following mixture-tuned matched filtering analysis of hyperspectral images. 5-fold zoom-ins (1 cm = 20 μm) of noise-free image data with superimposed classification results are shown. MS2 viruses appear as green pixels after staining with 2.5% phosphotungstic acid. $\text{C}_{60}(\text{NH}_2)_6$ is shown as red colour (a), aqu-n C_{60} as blue (b), $\text{C}_{60}(\text{OH})_6$ as purple (c), and $\text{C}_{60}(\text{OH})_{24}$ as pink (d). Corresponding TEM images after sample dehydration are shown in (e–h). Reproduced with permission from ref. ⁹⁶. Copyright 2012 American Chemical Society.

Inactivation of *MS2 bacteriophage* has been also demonstrated in the case of fullerene derivatives. Cationic amine-functionalized C_{60} derivatives⁹⁸, tris-adducted fulleropyrrolidinium aggregates⁹⁹ have shown a remarkable antiviral activity even if a direct comparison in terms of inactivation capability is difficult because of the different experimental conditions. A dependence of the inactivation efficacy on intensity of light and concentration of fullerenes has been observed⁸⁴.

Another possibility is using fullerenes to create a photoactive platform capable of remote inactivation of viruses and bacteria. A substrate of hot-pressed silica particles deposited on a metallic substrate has been functionalized with 3-aminopropyltriethoxysilane and the amine groups used to covalently attach the fullerenes¹⁰⁰. The inactivation of the *MS2 bacteriophage virus* has been studied at predefined distances from the irradiated surface. Inactivation of the virus via singlet oxygen has been observed to be effective up to around 10-15 cm from the surface (**Figure 15**).

Another important property to consider in developing an antiviral platform based on UV irradiation of fullerenes is their radical sinking effect¹⁰¹. This reduced the efficiency of binary systems formed by titania which upon UV irradiation generates free radicals and fullerenes which act as radical sinks.





View Article Online
DOI: 10.1039/D0SC02658A

Figure 15. (a) Electrospaying silica particles (dispersed in methanol) on stainless-steel mesh; (b) hot pressing; (c) amination of silica loaded on stainless-steel mesh with 3-aminopropyltriethoxysilane; (d) covalent C₆₀ attachment through nucleophilic addition of primary amines; and (e) use of C₆₀ immobilized on the amine-functionalized silica-coated stainless steel mesh for visible-light-sensitized remote singlet oxygenation. Reproduced with permission from ref. ¹⁰⁰. Copyright 2020 Elsevier Ltd.

5. A summary and a future outlook

The request for antiviral solutions has recently put the attention of the scientific community to innovative solutions. Nanomaterials, because the scale and surface properties can be specifically engineered, are potentially disruptive new antiviral tools. Many of these materials are already leading players in nanotechnology, with a key role in several research fields such as photocatalysis, photonics and optoelectronics. Metallic and oxide nanoparticles, in particular, have been widely tested as antiviral materials¹⁰², but several questions remain to be solved such as the cytotoxicity, which still needs to be fully assessed. This is the reason why we have not included in the present review another important class of carbon-based nanomaterials, the carbon nanotubes. Their potential toxicity still represents, in fact, a major issue. Carbon-based nanomaterials are, however, interesting candidates for antiviral applications, in particular graphene, carbon dots and fullerenes.

Table 1 shows a summary of the main carbon nanomaterials which have been tested as antivirals. The large variety of combinations suggest that the studies in this field are still in the exploratory phase and much work need to be addressed. In particular, an important general question which has to be studied and assessed is the relationship between the C-dots dimension and shape with that one of the virus. The possibility of fabricating C-dots that simulate the virus shape and surface is a very challenging issue but specific and systematic studies have to be carefully performed.



Table 1: Summary of Carbon-based nanomaterials as antiviralsView Article Online
DOI: 10.1039/D0SC02658A

Virus	Family	Species	Nucleic acid	Viral envelope	Carbon-based materials	Ref.
PEDV	Coronaviridae	Porcine epidemic diarrhea virus	RNA	enveloped	GO, C-dots	18, 52
FCoV		Alphacoronavirus 1			GO-AgNPs	30
HCoV-229E		Human coronavirus 229E			C-dots	53
SuHV-1 (PRV)	Herpesviridae	Suid alphaherpesvirus 1	DNA	enveloped	GO, C-dots	18, 50
HSV-1		Human alphaherpesvirus 1			GO, C-dots, GQDs, Fullerene	20,27,32, 34,38,48, 49, 64, 84
HCMV		Human betaherpesvirus 5			Fullerene	84
H9N2	Orthomyxoviridae	Influenza A	RNA	enveloped	GO	21
H1N1					Fullerene	81, 91, 95, 97
H3N2					-	-
H3N3					Fullerene	81
EV71	Picornaviridae	Enterovirus A	RNA	non-enveloped	GO, C-dots	21, 51
MS2 bacteriophage	Leviviridae	Escherichia virus	RNA	non-enveloped	GO, Fullerene	24-26, 96, 98,99
IBDV	Birnaviridae	Infectious Bursal disease virus	RNA	non-enveloped	GO-AgNPs	30
PRRSV	Arteriviridae	Betaarterivirus suid 1	RNA	enveloped	GO-AgNPs, C-dots	31, 50
VSV	Rhabdoviridae	Indiana vesicolorum	RNA	enveloped	GO	35



ASFV	Asfarviridae	African swine fever virus			TRGO-PG	32
HIV	Retroviridae		RNA	enveloped	G, Fullerene	36, 81
SIV					Fullerene	77
M-MuLV		Murine leukemia virus			Fullerene	77
NDRV	Reoviridae		RNA	non-enveloped	GO/HY	37
JEV	Flaviviridae	Japanese Encephalitis virus	RNA	enveloped	C-dots	54
ZIKV		Zika virus			C-dots, Fullerene	52, 85
DENV		Dengue virus			Fullerene	54, 85
HCV		Hepacivirus C			Fullerene	82
AAV	Parvoviridae	Adeno-associated dependoparvovirus	DNA	non-enveloped	C-dots	54
PPD		Ungulate protoparvovirus 1			C-dots	54
RSV	Pneumoviridae	Human orthopneumovirus	RNA	enveloped	GO, Fullerene	33,83

View Article Online
DOI: 10.1039/D0SC02658A

In addition to the carbon-based nanomaterials considered in this overview, it is worth mentioning the nanodiamonds which, with their particular surfaces and dimensions, are potential candidates of importance in nanomedicine. (ND)¹⁰³. NDs are among the smallest carbon-based materials and are, conventionally, crystalline nanoparticles of about 5 nm in size.¹⁰⁴ Their unique characteristics derive from the physico-chemical properties of the particle facets. NDs can be obtained by the detonation of explosive carbon-based materials. Some of the particles are crystalline carbon objects below 10 nm¹⁰⁵. This procedure suffers from several drawbacks, including the high quantity of purities that requires purification work. Among the most common impurities are metals and carbon-based systems with a different structure from that of the diamond. Over the years, numerous purification processes have been implemented, including oxidative treatments in the liquid or gaseous phase and acid treatments^{103,106–109}. One of the most severe drawbacks that can be encountered in the use of NDs is their tendency to aggregate, leading to the formation of clusters of hundreds of nanometres. This phenomenon is facilitated by the presence on the surface of functional groups (carboxylic, hydroxylic, etc.) capable of generating hydrogen or covalent bonds, determining high adhesion forces. NDs can be easily functionalized for specific biological applications. The surface

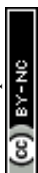


functional groups determine the chemical environment of use, the interaction with tissues, and can improve biocompatibility. Among post-synthesis processes, graphitization to obtain sp^2 carbon on the surface, hydrogenation, silanization and reactions with amines or PEG¹⁰³ are the most common. To date, no studies are investigating the antiviral activity of NDs. However, considerable efforts have been made to study the toxicological properties and biocompatibility of NDs. In particular, it has been demonstrated that purified NDs do not show significant toxicity. Ivanova et al.¹¹⁰ have reported the effects of NDs interaction with influenza viruses. This study highlighted the absorbency of NDs against viruses. Viruses such as influenza A H1N1 and H3N2 were concentrated and placed in a solution of NDs. Hemagglutination tests with erythrocytes were used for virus detection. Absorption and desorption studies have highlighted the possibility of using NDs as antimicrobial filters. NDs have shown encouraging results in attaching envelopes of *E. coli* and as antibacterial. The most promising results highlight that NDs have relevant properties as potential drug delivery systems, with numerous engineering and functionalization possibilities¹⁰⁴. As antiviral, the current literature does not show emerging opportunities and a greater effort has to be done to improve current knowledge about cytotoxicity and purification of such systems.

About the perspectives of graphene as antiviral material we also have to distinguish between graphene and graphene oxide. Graphene oxide has antibacterial activity and, to a lesser extent, also antiviral properties, well documented for pseudorabies viruses. However, the characteristics of low toxicity and surface functionalization allow thinking of graphene as a useful platform in combination with other antiviral systems acting on nanoscale. For this reason most of the experiments have used GO, to exploit the possibilities of surface functionalization. GO and graphene have high potentialities for virus detection but a direct use as antiviral is more difficult to forecast also because their dimension and shape are large in the nanoscale and difficult to control. However, to date, there are no systematic studies that allow achieving a clear identification of the antiviral mechanism, and specific studies have to be addressed to understand the graphene-virus interaction. It has been suggested that the antivirucidal activity is due to physical disruption of the virus by the sharp edge of graphene. It is not clear, however, if this mechanism is working in general or only for specific types of virus

Among the latest tested antiviral systems, carbon dots have shown encouraging results in terms of biocompatibility and antiviral properties. Carbon dots have many advantages. They can be easily synthesised from a few precursors through a process based on carbonisation. The surface of these nanomaterials can be properly engineered either in the synthesis phase through the choice of precursors or through a post-synthesis functionalization. The main problem with C-dots is the lack of a single model applicable to interaction with viruses. The variety of C-dots species is potentially endless and it is necessary to create a shortlist of few potential candidates to be tested for cytotoxicity and antiviral activity studies. To date, the literature is rich in a multiplicity of papers focused on the synthesis of carbon-based particles, lacking in a systematic investigations on the role of surfaces, size, shape and functional groups.

Despite the encouraging results, there is still much to be done for the use of carbon-based nanomaterials in nanomedicine. Although carbon dots have revealed significant antiviral activity, the success rate of most C-dots is remarkable in the early stages of the infection, when the nanoparticle seems to have a role in interfering with the interaction mechanism



between virion and cell. To date, one of the main obstacles to an improvement in antiviral properties against a specific virus is the lack of knowledge of the mechanism of action. In fact, as we have seen, the dependence of antiviral activity on some surface functional groups of the nanoparticle is contradictory and not fully demonstrated. Moreover, it is not clear whether C-dots are able to attack the virus directly, playing a virucidal role. Finally, there are many in vitro experiments, while the in vivo ones are still few and are necessary to know the real potential of such systems. Another advantage of C-dots is the possibility of tailored surface functionalization, but on the other hand their structure is only defined in terms of properties and a specific control is still difficult to achieve.

Fullerenes have also shown remarkable properties as antiviral nanosystems. They have the advantage, with respect to graphene and C-dots, to have a well-defined composition and shape and a well-established functionalization chemistry. Fullerenes have also widely studied as anti-HIV agents with promising results using different types of derivatives, but also in this case the cytotoxicity needs to be carefully evaluated. Fullerenes can generate a large amount of singlet oxygen which could be used to destroy the viruses and sanitize surfaces.

The exploration of antiviral properties and applications of carbon-based nanomaterials is still a new field and much research is still needed to assess the potentialities in the field. Carbon nanomaterials have, however, the potentiality to create antiviral systems with reduced toxicity. A full assessment of cytotoxicity appears the main issue to allow the development of antiviral applications for such class of materials.

References

- 1 V. Cagno, P. Andreozzi, M. D'Alicarnasso, P. J. Silva, M. Mueller, M. Galloux, R. Le Goffic, S. T. Jones, M. Vallino, J. Hodek, J. Weber, S. Sen, E. R. Janecek, A. Bekdemir, B. Sanavio, C. Martinelli, M. Donalisio, M. A. R. Welti, J. F. Eleouet, Y. Han, L. Kaiser, L. Vukovic, C. Tapparel, P. Král, S. Krol, D. Lembo and F. Stellacci, *Nat. Mater.*, 2018, **17**, 195–203.
- 2 P. P. Dechant, J. Wardman, T. Keef and R. Twarock, *Acta Crystallogr. Sect. A Found. Adv.*, 2014, **70**, 162–167.
- 3 A. a. Hassan, M. K. Mansour, R. M. H. Sayed El Ahl, A. M. a. El Hamaky and N. H. Oraby, *Toxic and beneficial effects of carbon nanomaterials on human and animal health*, Elsevier Inc., 2020.
- 4 A. Pinna, L. Malfatti, G. Galleri, R. Manetti, S. Cossu, G. Rocchitta, R. Migheli, P. A. Serra and P. Innocenzi, *RSC Adv.*, 2015, **5**, 20432–20439.
- 5 L. Pinna, Alessandra; Cali, Eleonora; Kerherve, Gwilherm; Galleri, Grazie; Maggini, Michele; Innocenzi, Plinio; Malfatti, *Nanoscale Adv.*
- 6 G. Chen, I. Roy, C. Yang and P. N. Prasad, *Chem. Rev.*, 2016, **116**, 2826–2885.
- 7 F. M. Tonelli, V. A. Goulart, K. N. Gomes, M. S. Ladeira, A. K. Santos, E. Lorençon, L. O. Ladeira and R. R. Resende, *Nanomedicine*, 2015, **10**, 2423–2450.



- 8 H. Roy, S. Bhanja, U. P. Panigrahy and V. K. Theendra, *Graphene-Based Nanovehicles for Drug Delivery*, Elsevier Inc., 2018. View Article Online
DOI: 10.1039/D0SC02658A
- 9 D. De Melo-Diogo, R. Lima-Sousa, C. G. Alves and I. J. Correia, *Biomater. Sci.*, 2019, **7**, 3534–3551.
- 10 O. Akhavan, *Graphene scaffolds in progressive nanotechnology/stem cell-based tissue engineering of the nervous system*, 2016, vol. 4.
- 11 L. Shang, Y. Qi, H. Lu, H. Pei, Y. Li, L. Qu, Z. Wu and W. Zhang, *Graphene and graphene oxide for tissue engineering and regeneration*, Elsevier Inc., 2019.
- 12 D. Du, Y. Yang and Y. Lin, *MRS Bull.*, 2012, **37**, 1290–1296.
- 13 J. Lin, X. Chen and P. Huang, *Adv. Drug Deliv. Rev.*, 2016, **105**, 242–254.
- 14 W. Hu, C. Peng, W. Luo, M. Lv, X. Li, D. Li, Q. Huang and C. Fan, *ACS Nano*, 2010, **4**, 4317–4323.
- 15 S. Liu, T. H. Zeng, M. Hofmann, E. Burcombe, J. Wei, R. Jiang, J. Kong and Y. Chen, *ACS Nano*, 2011, **5**, 6971–6980.
- 16 O. Akhavan and E. Ghaderi, *ACS Nano*, 2010, **4**, 5731–5736.
- 17 C. Lee., *Virol. J.*, 2015, **12**:193
- 18 S. Ye, K. Shao, Z. Li, N. Guo, Y. Zuo, Q. Li, Z. Lu, L. Chen, Q. He and H. Han, *ACS Appl. Mater. Interfaces*, 2015, **7**, 21578–21579.
- 19 L. E. Pomeranz, A. E. Reynolds and C. J. Hengartner, *Microbiol. Mol. Biol. Rev.*, 2005, **69**, 462–500.
- 20 M. Sametband, I. Kalt, A. Gedanken and R. Sarid, *ACS Appl. Mater. Interfaces*, 2014, **6**, 1228–1235.
- 21 Z. Song, X. Wang, G. Zhu, Q. Nian, H. Zhou, D. Yang, C. Qin and R. Tang, *Small*, 2015, **11**, 1771–1776.
- 22 J. B. Ge, R. Pokhrel, N. Bhattarai, K. a. Johnson, B. S. Gerstman, R. V. Stahelin and P. P. Chapagain, *Biochem. Biophys. Res. Commun.*, 2017, **493**, 176–181.
- 23 K. Krishnamoorthy, R. Mohan and S. J. Kim, *Appl. Phys. Lett.*, 2011, **24**, 2013-2016.
- 24 X. Hu, L. Mu, J. Wen and Q. Zhou, *Carbon N. Y.*, 2012, **50**, 2772–2781.
- 25 K. Valegård, L. Liljas, K. Fridborg and T. Unge, *Nature*, 1990, **345**, 36–41.
- 26 O. Akhavan, M. Choobtashani and E. Ghaderi, *J. Phys. Chem. C*, 2012, **116**, 9653–9659.



- 27 J. L. Elechiguerra, J. L. Burt, J. R. Morones, A. Camacho-Bragado, X. Gao, H. Lara and M. J. Yacaman, *J. Nanobiotechnology*, 2005, **3**, 1–10. View Article Online
DOI:10.1039/D0SC02658A
- 28 L. Liu, J. Liu, Y. Wang, X. Yan and D. D. Sun, *New J. Chem.*, 2011, **35**, 1418–1423.
- 29 S. Jaworski, M. Wierzbicki, E. Sawosz, A. Jung, G. Gielerak, J. Biernat, H. Jaremek, W. Łojkowski, B. Woźniak, J. Wojnarowicz, L. Stobiński, A. Małolepszy, M. Mazurkiewicz-Pawlicka, M. Łojkowski, N. Kurantowicz and A. Chwalibog, *Nanoscale Res. Lett.*, 2018, **13**:116.
- 30 Y. N. Chen, Y. H. Hsueh, C. Te Hsieh, D. Y. Tzou and P. L. Chang, *Int. J. Environ. Res. Public Health*, 2016, **4**, 4-6 , DOI:10.3390/ijerph13040430.
- 31 T. Du, J. Lu, L. Liu, N. Dong, L. Fang, S. Xiao and H. Han, *ACS Appl. Bio Mater.*, 2018, **1**, 1286–1293.
- 32 B. Ziem, J. Rahn, I. Donskyi, K. Silberreis, L. Cuellar, J. Dervedde, G. Keil, T. C. Mettenleiter and R. Haag, *Macromol. Biosci.*, 2017, **17**, 1–9.
- 33 X. X. Yang, C. M. Li, Y. F. Li, J. Wang and C. Z. Huang, *Nanoscale*, 2017, **9**, 16086–16092.
- 34 I. S. Donskyi, W. Azab, J. L. Cuellar-Camacho, G. Guday, A. Lippitz, W. E. S. Unger, K. Osterrieder, M. Adeli and R. Haag, *Nanoscale*, 2019, **11**, 15804–15809.
- 35 M. F. Gholami, D. Lauster, K. Ludwig, J. Storm, B. Ziem, N. Severin, C. Böttcher, J. P. Rabe, A. Herrmann, M. Adeli and R. Haag, *Adv. Funct. Mater.*, 2017, **27**, 1–12.
- 36 N. K. Rathinam, C. Saravanan, P. Parimal, V. Perumal and M. Perumal, *Korean J. Chem. Eng.*, 2014, **31**, 744–747.
- 37 X. Du, R. Xiao, H. Fu, Z. Yuan, W. Zhang, L. Yin, C. He, C. Li, J. Zhou, G. Liu, G. Shu and Z. Chen, *Mater. Sci. Eng. C*, 2019 , **105**: 110052.
- 38 A. R. Deokar, A. P. Nagvenkar, I. Kalt, L. Shani, Y. Yeshurun, A. Gedanken and R. Sarid, *Bioconjug. Chem.*, 2017, **28**, 1115–1122.
- 39 M. C. Wu, A. R. Deokar, J. H. Liao, P. Y. Shih and Y. C. Ling, *ACS Nano*, 2013, **7**, 1281–1290.
- 40 J. Ge, M. Lan, B. Zhou, W. Liu, L. Guo, H. Wang, Q. Jia, G. Niu, X. Huang, H. Zhou, X. Meng, P. Wang, C. S. Lee, W. Zhang and X. Han, *Nat. Commun.*, 2014, **5**, 1–8.
- 41 P. Innocenzi, L. Malfatti and D. Carboni, *Nanoscale*, 2015, **7**, 12759–12772.
- 42 Carbonaro, Corpino, Salis, Mocci, Thakkar, Olla and Ricci, *C — J. Carbon Res.*, 2019, **5**, 60.



- 43 A. Sharma and J. Das, *J. Nanobiotechnology*, 2019, **17**, 1–24. View Article Online
DOI: 10.1039/D0SC02658A
- 44 R. Ludmerczki, S. Mura, C. M. Carbonaro, I. M. Mandity, M. Carraro, N. Senes, S. Garroni, G. Granozzi, L. Calvillo, S. Marras, L. Malfatti and P. Innocenzi, *Chem. - A Eur. J.*, 2019, **25**, 11963–11974.
- 45 K. Suzuki, L. Malfatti, M. Takahashi, D. Carboni, F. Messina, Y. Tokudome, M. Takemoto and P. Innocenzi, *Sci. Rep.*, 2017, **7**, 1–11.
- 46 T. Tong, H. Hu, J. Zhou, S. Deng, X. Zhang, W. Tang, L. Fang, S. Xiao and J. Liang, *Small*, 2020, **16**, 1–12.
- 47 M. Khanal, A. Barras, T. Vausselin, L. Fénéant, R. Boukherroub, A. Siriwardena, J. Dubuisson and S. Szunerits, *Nanoscale*, 2015, **7**, 1392–1402.
- 48 A. Barras, Q. Pagneux, F. Sane, Q. Wang, R. Boukherroub, D. Hober and S. Szunerits, *ACS Appl. Mater. Interfaces*, 2016, **8**, 9004–9013.
- 49 M. Z. Fahmi, W. Sukmayani, S. Q. Khairunisa, a. M. Witaningrum, D. W. Indriati, M. Q. Y. Matondang, J. Y. Chang, T. Kotaki and M. Kameoka, *RSC Adv.*, 2016, **6**, 92996–93002.
- 50 T. Du, J. Liang, N. Dong, L. Liu, L. Fang, S. Xiao and H. Han, *Carbon N. Y.*, 2016, **110**, 278–285.
- 51 C. J. Lin, L. Chang, H. W. Chu, H. J. Lin, P. C. Chang, R. Y. L. Wang, B. Unnikrishnan, J. Y. Mao, S. Y. Chen and C. C. Huang, *Small*, 2019, **15**, 1–14.
- 52 D. Ting, N. Dong, L. Fang, J. Lu, J. Bi, S. Xiao and H. Han, *ACS Appl. Nano Mater.*, 2018, **1**, 5451–5459.
- 53 A. Łoczechin, K. Séron, A. Barras, E. Giovanelli, S. Belouzard, Y. T. Chen, N. Metzler-Nolte, R. Boukherroub, J. Dubuisson and S. Szunerits, *ACS Appl. Mater. Interfaces*, 2019, **11**, 42964–42974.
- 54 S. Huang, J. Gu, J. Ye, B. Fang, S. Wan, C. Wang, U. Ashraf, Q. Li, X. Wang, L. Shao, Y. Song, X. Zheng, F. Cao and S. Cao, *J. Colloid Interface Sci.*, 2019, **542**, 198–206.
- 55 X. Dong, M. M. Moyer, F. Yang, Y. P. Sun and L. Yang, *Sci. Rep.*, 2017, **7**, 1–10.
- 56 K. Joshi, B. Mazumder, P. Chattopadhyay, N. S. Bora, D. Goyary and S. Karmakar, *Curr. Drug Deliv.*, 2018, **16**, 195–214.
- 57 M. Li, T. Chen, J. J. Gooding and J. Liu, *ACS Sensors*, 2019, **4**, 1732–1748.
- 58 Y. Yan, J. Gong, J. Chen, Z. Zeng, W. Huang, K. Pu, J. Liu and P. Chen, *Adv. Mater.*, 2019, **31**, 1–22.



- 59 S. Tajik, Z. Dourandish, K. Zhang, H. Beitollahi, Q. Van Le, H. W. Jang and M. Shokouhimehr, *RSC Adv.*, 2020, **10**, 15406–15429. View Article Online
DOI: 10.1039/D0SC02658A
- 60 S. Zhu, Q. Meng, L. Wang, J. Zhang, Y. Song, H. Jin, K. Zhang, H. Sun, H. Wang and B. Yang, *Angew. Chemie - Int. Ed.*, 2013, **52**, 3953–3957.
- 61 K. Ghanbari, M. Roushani and A. Azadbakht, *Anal. Biochem.*, 2017, **534**, 64–69.
- 62 Q. Xiang, J. Huang, H. Huang, W. Mao and Z. Ye, *RSC Adv.*, 2018, **8**, 1820–1825.
- 63 M. L. Chen, Y. J. He, X. W. Chen and J. H. Wang, *Bioconjug. Chem.*, 2013, **24**, 387–397.
- 64 D. Iannazzo, A. Pistone, S. Ferro, L. De Luca, A. M. Monforte, R. Romeo, M. R. Buemi and C. Pannecouque, *Bioconjug. Chem.*, 2018, **29**, 3084–3093.
- 65 J. Du, B. Feng, Y. Dong, M. Zhao and X. Yang, *Nanoscale*, 2020, **12**, 9219–9230.
- 66 M. Prato, *J. Mater. Chem.*, 1997, **7**, 1097–1109.
- 67 S. H. Friedman, D. L. Decamp and G. L. Kenyon, 1993, 6510–6512.
- 68 E. Castro, Z. S. Martinez, C. S. Seong, A. Cabrera-Espinoza, M. Ruiz, A. Hernandez Garcia, F. Valdez, M. Llano and L. Echegoyen, *J. Med. Chem.*, 2016, **59**, 10963–10973.
- 69 G. Luca Marcorin, T. Da Ros, S. Castellano, G. Stefancich, I. Bonin, S. Miertus and M. Prato, *Org. Lett.*, 2000, **2**, 3955–3957.
- 70 A. Barzegar, S. Jafari Mousavi, H. Hamidi and M. Sadeghi, *Phys. E Low-Dimensional Syst. Nanostructures*, 2017, **93**, 324–331.
- 71 Z. S. Martinez, E. Castro, C. S. Seong, M. R. Cerón, L. Echegoyen and M. Llano, *Antimicrob. Agents Chemother.*, 2016, **60**, 5731–5741.
- 72 H. Yilmaz, L. Ahmed, B. Rasulev and J. Leszczynski, *J. Nanoparticle Res.*, , DOI:10.1007/s11051-016-3429-7.
- 73 N. a. Saleh, *Spectrochim. Acta - Part A Mol. Biomol. Spectrosc.*, 2015, **136**, 1523–1529.
- 74 K. A. Khadra, S. Mizyed, D. Marji, S. F. Haddad, M. Ashram and A. Foudeh, *Spectrochim. Acta - Part A Mol. Biomol. Spectrosc.*, 2015, **136**, 1869–1874.
- 75 S. Marchesan, T. Da Ros, G. Spalluto, J. Balzarini and M. Prato, *Bioorganic Med. Chem. Lett.*, 2005, **15**, 3615–3618.
- 76 S. Promsri, P. Chuichay, V. Sanghiran, V. Parasuk and S. Hannongbua, *J. Mol. Struct. THEOCHEM*, 2005, **715**, 47–53.



- 77 J. Nacsa, J. Segesdi, Á. Gyuris, T. Braun, H. Rausch, Á. Buvári-Barcza, L. Barcza, J. Minarovits and J. Molnár, *Fuller. Sci. Technol.*, 1997, **5**, 969–976. View Article Online
DOI: 10.1039/D0SC02658A
- 78 R. F. Rhule, J.T.; Hill, C.L.; Zheng, Z.; Schinazi, in *Metallopharmaceuticals II. Topics in Biological Inorganic Chemistry, vol 2.*, Springer Berlin Heidelberg, 1999, pp. 117–137.
- 79 E. Nakamura and H. Isobe, *Acc. Chem. Res.*, 2003, **36**, 807–815.
- 80 O. a. Troshina, P. a. Troshin, A. S. Peregudov, V. I. Kozlovskiy, J. Balzarini and R. N. Lyubovskaya, *Org. Biomol. Chem.*, 2007, **5**, 2783–2791.
- 81 A. B. Kornev, A. S. Peregudov, V. M. Martynenko, J. Balzarini, B. Hoorelbeke and P. a. Troshin, *Chem. Commun.*, 2011, **47**, 8298–8300.
- 82 H. Kataoka, T. Ohe, K. Takahashi, S. Nakamura and T. Mashino, *Bioorganic Med. Chem. Lett.*, 2016, **26**, 4565–4567.
- 83 I. N. Falynskova, K. S. Ionova, a. V. Dedova, I. a. Leneva, N. R. Makhmudova and L. D. Rasnetsov, *Pharm. Chem. J.*, 2014, **48**, 85–88.
- 84 N. E. Fedorova, R. R. Klimova, Y. a. Tulenev, E. V. Chichev, A. B. Kornev, P. a. Troshin and A. a. Kushch, *Mendeleev Commun.*, 2012, **22**, 254–256.
- 85 J. Ramos-Soriano, J. J. Reina, B. M. Illescas, N. De La Cruz, L. Rodríguez-Pérez, F. Lasala, J. Rojo, R. Delgado and N. Martín, *J. Am. Chem. Soc.*, 2019, **141**, 15403–15412.
- 86 J. W. Arbogast, A. P. Darmanyan, C. S. Foote, Y. Rubin, F. N. Diederich, M. M. Alvarez, S. J. Anz and R. L. Whetten, *J. Phys. Chem.*, 1991, **95**, 11–12.
- 87 D. R. Kearns, *Chem. Rev.*, 1971, **71**, 395–427.
- 88 I. V. Bagrov, I. M. Belousova, V. M. Kiselev and I. M. Kislyakov, *J. Opt. Technol.*, 2019, **86**, 66.
- 89 L. Brunet, D. Y. Lyon, E. M. Hotze, P. J. J. Alvarez and M. R. Wiesner, *Environ. Sci. Technol.*, 2009, **43**, 4355–4360.
- 90 J. Lee, S. Hong, Y. MacKeyev, C. Lee, E. Chung, L. J. Wilson, J. H. Kim and P. J. J. Alvarez, *Environ. Sci. Technol.*, 2011, **45**, 10598–10604.
- 91 J. Lenard and R. Vanderoef, *Photochem. Photobiol.*, 1993, **58**, 527–531.
- 92 F. Käsermann and C. Kempf, *Antiviral Res.*, 1997, **34**, 65–70.
- 93 F. Käsermann and C. Kempf, *Rev. Med. Virol.*, 1998, **8**, 143–151.
- 94 Y. Rud, S. Prylutska, L. Buchatskyy, Y. Prylutsky, U. Ritter and P. Scharff, *Materwiss. Werksttech.*, 2011, **42**, 136–138.



- 95 V. V. Zarubaev, I. M. Belousova, O. I. Kiselev, L. B. Piotrovsky, P. M. Anfimov, T. C. Krisko, T. D. Muraviova, V. V. Rylkov, A. M. Starodubzev and A. C. Sirotkin, *Photodiagnosis Photodyn. Ther.*, 2007, **4**, 31–35. View Article Online
DOI: 10.1039/7D0SC02658A
- 96 A. R. Badireddy, J. F. Budarz, S. Chellam and M. R. Wiesner, *Environ. Sci. Technol.*, 2012, **46**, 5963–5970.
- 97 I. M. Belousova, I. M. Kislyakov, T. D. Muraviova, a. M. Starodubtsev, T. K. Kris'ko, E. a. Selivanov, N. P. Sivakova, I. S. Golovanova, S. D. Volkova, a. a. Shtro and V. V. Zarubaev, *Photodiagnosis Photodyn. Ther.*, 2014, **11**, 165–170.
- 98 M. Cho, J. Lee, Y. MacKeyev, L. J. Wilson, P. J. J. Alvarez, J. B. Hughes and J. H. Kim, *Environ. Sci. Technol.*, 2010, **44**, 6685–6691.
- 99 S. D. Snow, K. Park and J. H. Kim, *Environ. Sci. Technol. Lett.*, 2014, **1**, 290–294.
- 100 J. Kim, H. Lee, J. Y. Lee, K. H. Park, W. Kim, J. H. Lee, H. J. Kang, S. W. Hong, H. J. Park, S. Lee, J. H. Lee, H. D. Park, J. Y. Kim, Y. W. Jeong and J. Lee, *Appl. Catal. B Environ.*, 2020, **270**:118862.
- 101 A. Pinna, L. Malfatti, M. Piccinini, P. Falcaro and P. Innocenzi, *J. Synchrotron Radiat.*, 2012, **19**, 586–590.
- 102 L. Chen and J. Liang, *Mater. Sci. Eng. C*, 2020, **112**, 110924.
- 103 K. Turcheniuk and V. N. Mochalin, *Nanotechnology*, , DOI:10.1088/1361-6528/aa6ae4.
- 104 A. M. Schrand, S. A. C. Hens and O. a. Shenderova, *Crit. Rev. Solid State Mater. Sci.*, 2009, **34**, 18–74.
- 105 L. Wang, Z. Yuan, H. E. Karahan, Y. Wang, X. Sui, F. Liu and Y. Chen, *Nanoscale*, 2019, **11**, 9819–9839.
- 106 S. J. Yu, M. W. Kang, H. C. Chang, K. M. Chen and Y. C. Yu, *J. Am. Chem. Soc.*, 2005, **127**, 17604–17605.
- 107 J. T. Paci, H. B. Man, B. Saha, D. Ho and G. C. Schatz, *J. Phys. Chem. C*, 2013, **117**, 17256–17267.
- 108 D. Mitev, R. Dimitrova, M. Spassova, C. Minchev and S. Stavrev, *Diam. Relat. Mater.*, 2007, **16**, 776–780.
- 109 I. Petrov, O. Shenderova, V. Grishko, V. Grichko, T. Tyler, G. Cunningham and G. McGuire, *Diam. Relat. Mater.*, 2007, **16**, 2098–2103.
- 110 V. T. Ivanova, M. V. Ivanova, B. V. Spitsyn, K. O. Garina, S. V. Trushakova, a. a. Manykin, a. P. Korzhenevsky and E. I. Burseva, *J. Phys. Conf. Ser.*, 2012, 345: 012019.



Open Access Article. Published on 16 June 2020. Downloaded on 6/23/2020 5:23:54 PM.
This article is licensed under a Creative Commons Attribution-NonCommercial 3.0 Unported Licence.

